TOKAPOLE II DESIGN

by

J. C. Sprott

T. W. Lovell

PLP 744

March 1978

Plasma Studies

University of Wisconsin

TOKAPOLE II DESIGN

Table of Contents

TOKAPOLE II DESIGN

PLP 730

J. C. Sprott, T. W. Lovell

I. INTRODUCTION

This PLP will explain the physics and engineering considerations that led to the design of Tokapole II. The goal was to produce a device that would give another 10 years of plasma physics relevant to the fusion program. The strategy was to build it enough like the small octupole that we could rely on our 13 years of experience to optimize the device, but sufficiently different that it would open new parameter regimes for study. The primary design criteria were simplicity, reliability, versatility, and economy. It was to perform as an octupole at least as well as its predecessor, but also to push as far as possible toward state-of-the-art Tokamak densities and temperatures. The expectation of hot, dense plasmas was based on extrapolation from the results obtained during six months of operation of the original small octupole with strong toroidal ohmic heating (the Tokapole I mode of operation). The major improvements dictated by the physics of tokapole operation were:

1) A larger minor radius and lower aspect ratio.

2) A stronger toroidal field of longer duration.

3) A higher degree of magnetic symmetry, especially the octupole null degeneracy.

4) An improved vacuum through better pumping, cleaner surfaces, and provisions for baking and discharge cleaning.

At the same time a large number of improvements were desired in order to improve access, reduce maintenance, and facilitate future modifications. It turned out that the above conditions could be most economically satisfied by preserving the existing iron core, control circuits, and diagnostics, but manufacturing a new vacuum vessel (including internal rings and toroidal and poloidal field coils), buying new vacuum pumps, and enlarging the existing capacitor banks (incorporating 54kJ of capacitors left over from the toroidal quadrupole). The parameters of the device are summarized in Table I.

II. VACUUM VESSEL

Conventional wisdom (see, for example, M. B. Gottlieb in PPPL-1296, Nov. 1976) holds that tokamak densities scale as $n \propto B_T/R_o$ where B_T is the toroidal magnetic field and R_o is the major radius, and that energy confinement times scale as $\tau \propto na^2$, where a is the minor radius. The product $n\tau$ is therefore proportional to $(B_T a/R_o)^2$, so that large toroidal fields and low aspect ratios (R_o/a) are desired. The existing iron core with a 10-inch square cross-section and a 28-inch square window was sufficient to allow a toroid with R_o = 50 cm. and a 44 cm. square cross-section with a reasonable allowance for wall thickness, toroidal field windings, continuity windings, poloidal field windings, and insulation.

A conducting wall is possible because the energy confinement time of tokamaks of this size and field ($B_T \lesssim$ 10 kG) is only ~1 msec. A high conductivity wall is also desirable in order to enhance equilibrium and stability as well as to smooth out field errors from the necessarily non-uniform winding of the toroidal and poloidal field coils. Of the available high conductivity materials, silver and copper were eliminated for economic reasons. Pure (1100) aluminum was also unavailable in the size and quantity required and was also undesirable because of its low yield strength and poor machinability. Type 6061-T6 aluminum was chosen as the best compromise of cost ($5,280), yield strength (40,000 psi), and conductivity (45% IACS). A thickness of 3 cm. was chosen so as to give a penetration time (defined by $\tau = 1/\omega$ where ω is the frequency at which the skin depth δ is equal to the thickness) of ~15 msec. The stresses produced by a 10 kG field were found to be acceptable for such a 3 cm.

TABLE I.

PARAMETERS OF TOKAPOLE II

MAJOR RADIUS: 50 CM

MINOR CROSS SECTION: 44 CM X 44 CM SQUARE

TOROID WALLS: ALUMINUM, 3.0 CM THICK WITH POLOIDAL AND TOROIDAL INSULTATED GAPS

VACUUM VOLUME: 600 LITERS

VACUUM SURFACE AREA: 6 SQUARE METERS

NUMBER OF INTERNAL RINGS: 4 (COPPER, 5 CM DIA., SUPPORTED AT 3 POINTS)

PORTS: 2-7.5" DIA., 5-4.5" DIA., 22-1.5" DIA., 13-0.25" DIA.

B_T ON AXIS: 4.4 KG (EXTENDABLE TO 10 KG BY THE ACQUISITION OF ADDITIONAL CAPACITORS)

L/R TIME OF B_T: 20 MSEC.

AVAILABLE OH VOLTAGE: 125 VOLTS

POLOIDAL FLUX: 0.15 WEBERS

AVAILABLE ENERGY (POLOIDAL + TOROIDAL FIELDS): 219 KJ (73-240μF, 5 KV CAPACITORS)

BASE VACUUM: 1×10^{-8} TORR

PUMPING SYSTEM: 1500ℓ/SEC TURBOMOLECULAR PUMP, 1000 ℓ/SEC 10° K CRYOPUMP, TITANIUM GETTER PUMP.

BAKEOUT TEMPERATURE: 150° C., QUICK COOL TO <50° C. IN 15 MIN.

PREIONIZATION: 5 KW, 2.45 GHZ; 10 KW, 9 GHZ; 10 KW, 16 GHZ ECRH thick wall. A square cross section without gussets was decided upon as a matter of simplicity and economy, and because magnetic flux calculations (to be described later) looked satisfactory. The tank was designed without an antigap to minimize field errors and to liberate room for ports and toroidal windings. The bottom was welded to the walls to insure good electrical conductivity as necessary to avoid toroidal field errors. The top, side, and bottom views of the vacuum tank are shown respectively in figs. 1-3.

Ports were laid out along radials at 30° intervals so that the toroidal field coil channels could be as straight and short as possible. Note that since the wall is thick and electrically conducting, toroidal field symmetry is assured if the toroidal field windings cross the gap at the outer lid flange at evenly spaced intervals, and this was done with considerable care. Wherever possible, symmetry about the horizontal midplane was preserved by arranging ports in pairs on the top and bottom. Two 6" ASA standard ports (7.5" clearance) were provided for pumps initially envisioned to be a 1500 ℓ/sec turbomolecular pump and a 1000 ℓ/sec, 10° K cryopump. The field errors produced by these necessarily large holes can later be minimized by installing 55% transparent copper plugs which would have an average resistivity equal to that of 6061 aluminum with a corresponding reduction in pumping speed. Two 4.5" diameter ports were placed in the lid directly above the pump ports, and three 4.5" diameter ports were provided at 120° intervals on the outer wall to provide access to most of the machine interior. A detailed list of the ports and their locations are given in Table II. In Table II, T refers to top, B to bottom, S to side, UO to upper outer hoop, etc., and the numbers refer to the azimuthal angle measured counterclockwise from the transformer core, as viewed from above. The positions of the ports on the outer wall are shown in fig. 4, and the detail of the ports is shown in fig. 5.

Poloidal and toroidal gaps were insulated with ¼" Viton sheet squeezed to a thickness of 0.180". The thickness was considered adequate to prevent arcs but not so great as to cause objectional field errors. Viton was considered satisfactory as

Figure 1

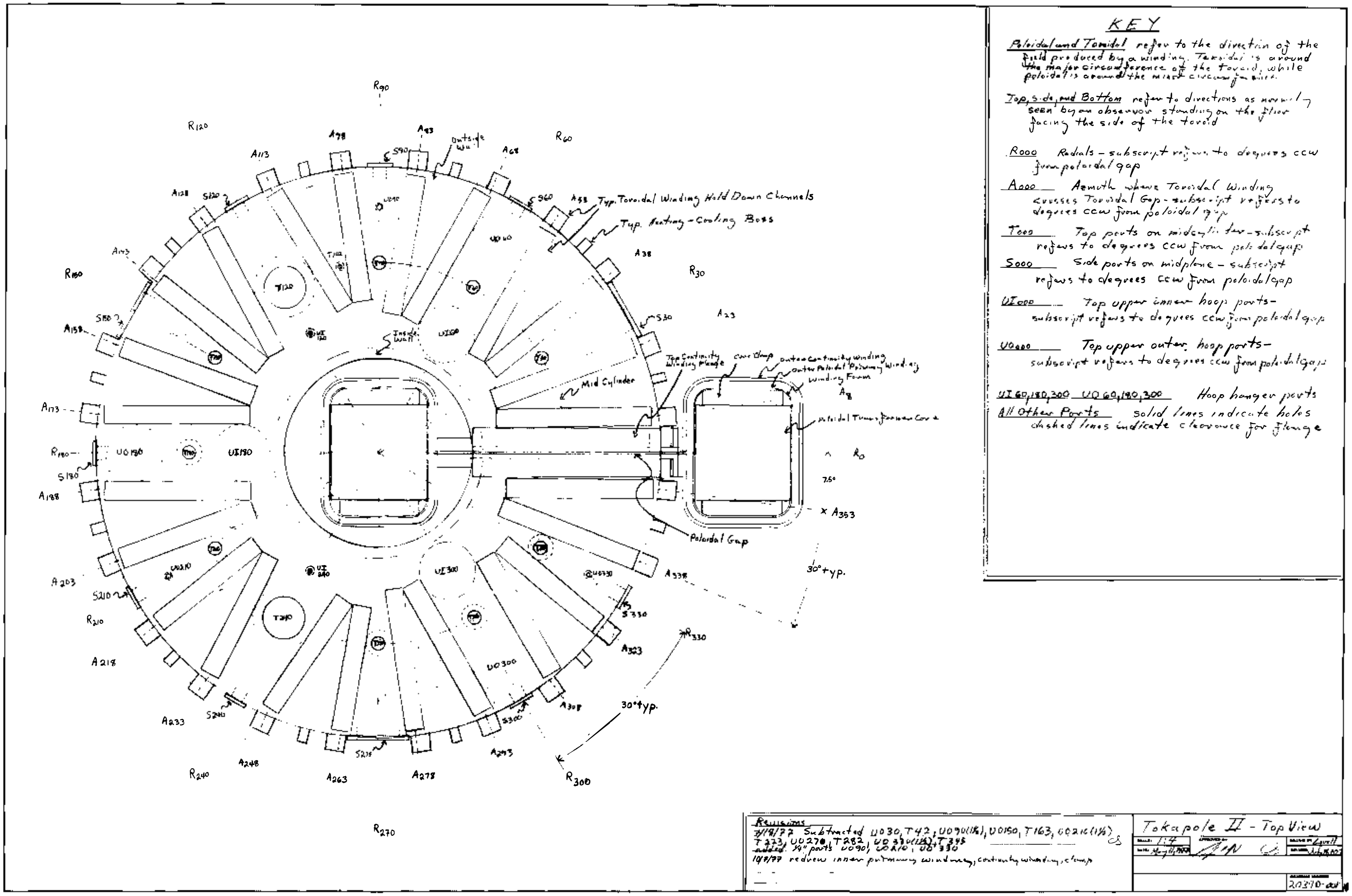
KEY
Poloidal and Toroidal refer to the direction of the field produced by a winding. Toroidal is around the major circumference of the toroid, while poloidal is around the minor circumference.
Top, side, and Bottom refer to directions as normally seen by an observer standing on the floor facing the side of the toroid
R000 Radials – subscript refers to degrees ccw from poloidal gap
A000 Azmuth where Toroidal Winding crosses Toroidal Gap – subscript refers to degrees ccw from poloidal gap
T000 Top ports on midcylinder – subscript refers to degrees ccw from poloidal gap
S000 Side ports on midplane – subscript refers to degrees ccw from poloidal gap
UI000 Top upper inner hoop ports – subscript refers to degrees ccw from poloidal gap
UO000 Top upper outer hoop ports – subscript refers to degrees ccw from poloidal gap
UI 60,180,300 UO 60,180,300 Hoop hanger ports
All Other Ports solid lines indicate holes dashed lines indicate clearance for flange
Typ. Toroidal Winding Hold Down Channels
Typ. Heating-Cooling Boss
Mid Cylinder
Poloidal Gap
Poloidal Transformer Core
30° typ.
Revisions
7/19/77 Subtracted UO30, T42, UO90(1½), UO150, T163, UO210(1½) T223, UO270, T282, UO330(1½), T345
added ¼" ports UO90, UO210, UO330
10/7/77 redraw inner primary winding, continuity winding, clamp
Tokapole II - Top View
1:4
20370-00

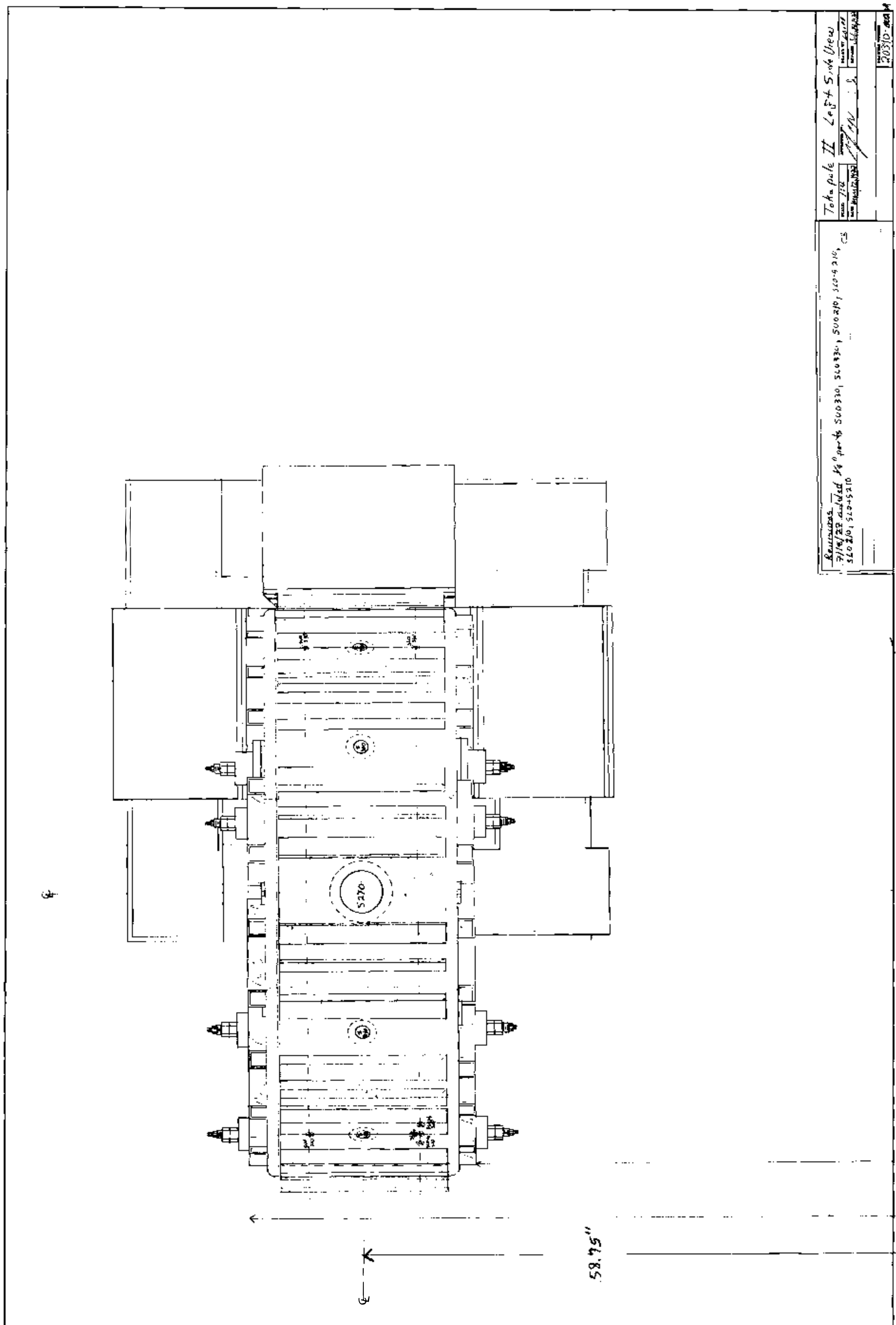

Figure 2

Figure 3

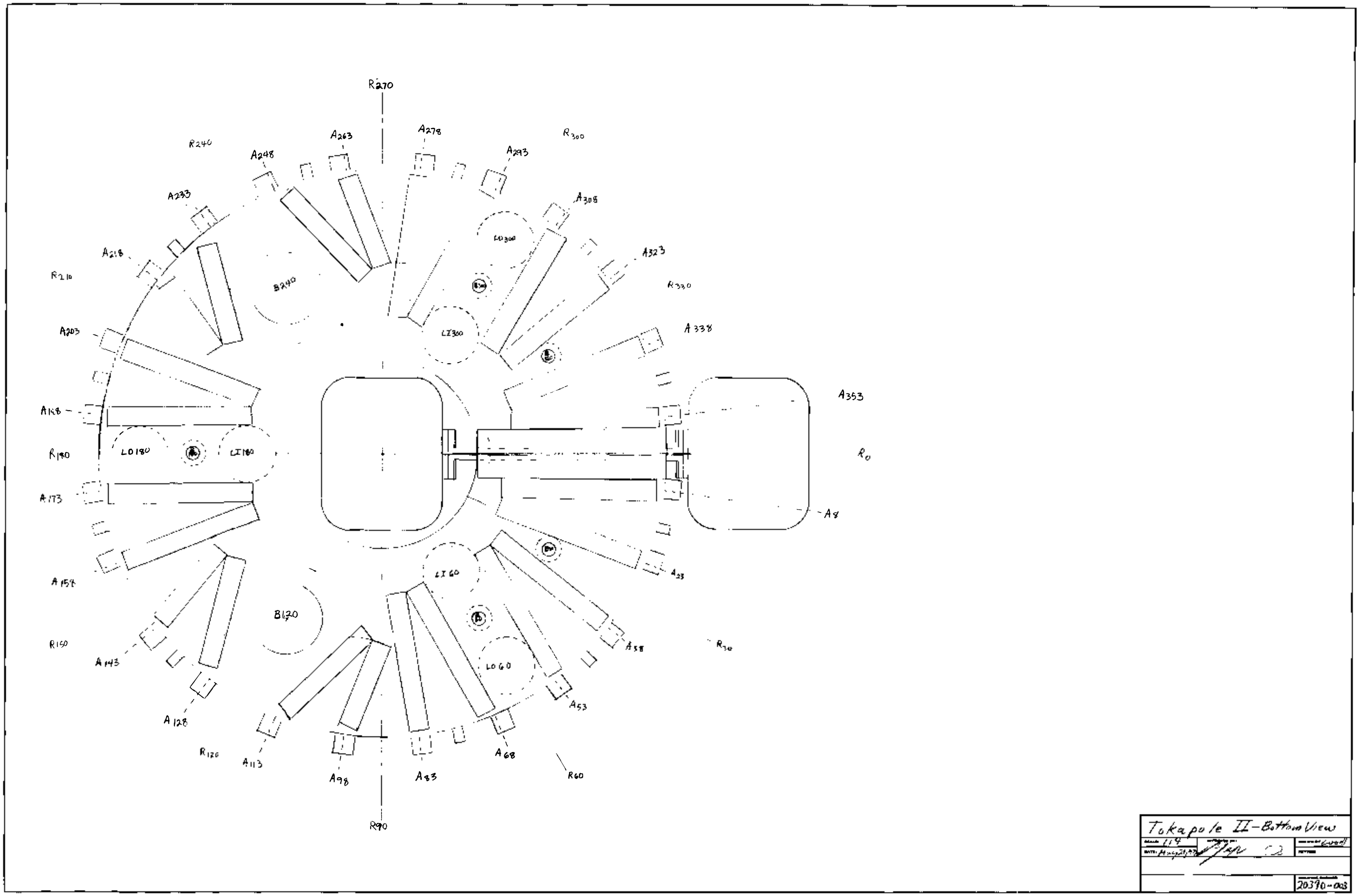

R270
R240
R300
R210
R330
R180
R0
R150
R30
R120
R60
R90
A263
A248
A278
A293
A233
A308
A218
A323
A203
A338
A188
A353
A173
A8
A158
A23
A143
A38
A128
A53
A113
A68
A98
A83
B240
B120
LO300
LI300
LO180
LI180
LI60
LO60
Tokapole II-Bottom View
20390-003

TABLE II.

TOKAPOLE II PORTS

7.5" (6" ASA) PORTS:

B 120

B 240

4.5" PORTS:

T 120

T 240

S 30

S 150

S 270

1.5" PORTS:

T 30

T 60

T 90

T 150

T 180

T 210

T 270

T 300

T 330

S 60

S 90

S 120

S 180

1.5" PORTS (CONT.):

S 210

S 240

S 300

S 330

B 30

B 60

B 180

B 300

B 330

HANGER PORTS:

UI 60

UO 60

UI 180

UO 180

UI 300

UO 300

LI 60

LO 60

LI 180

LO 180

LI 300

LO 300

0.25" PORTS:

UO 90

UI 120

UO 210

UI 240

UO 330

SUO 90

SLO 90

SUO 210

SLO 210

SLO-5 210

SLO+5 210

SUO 330

SLO 330

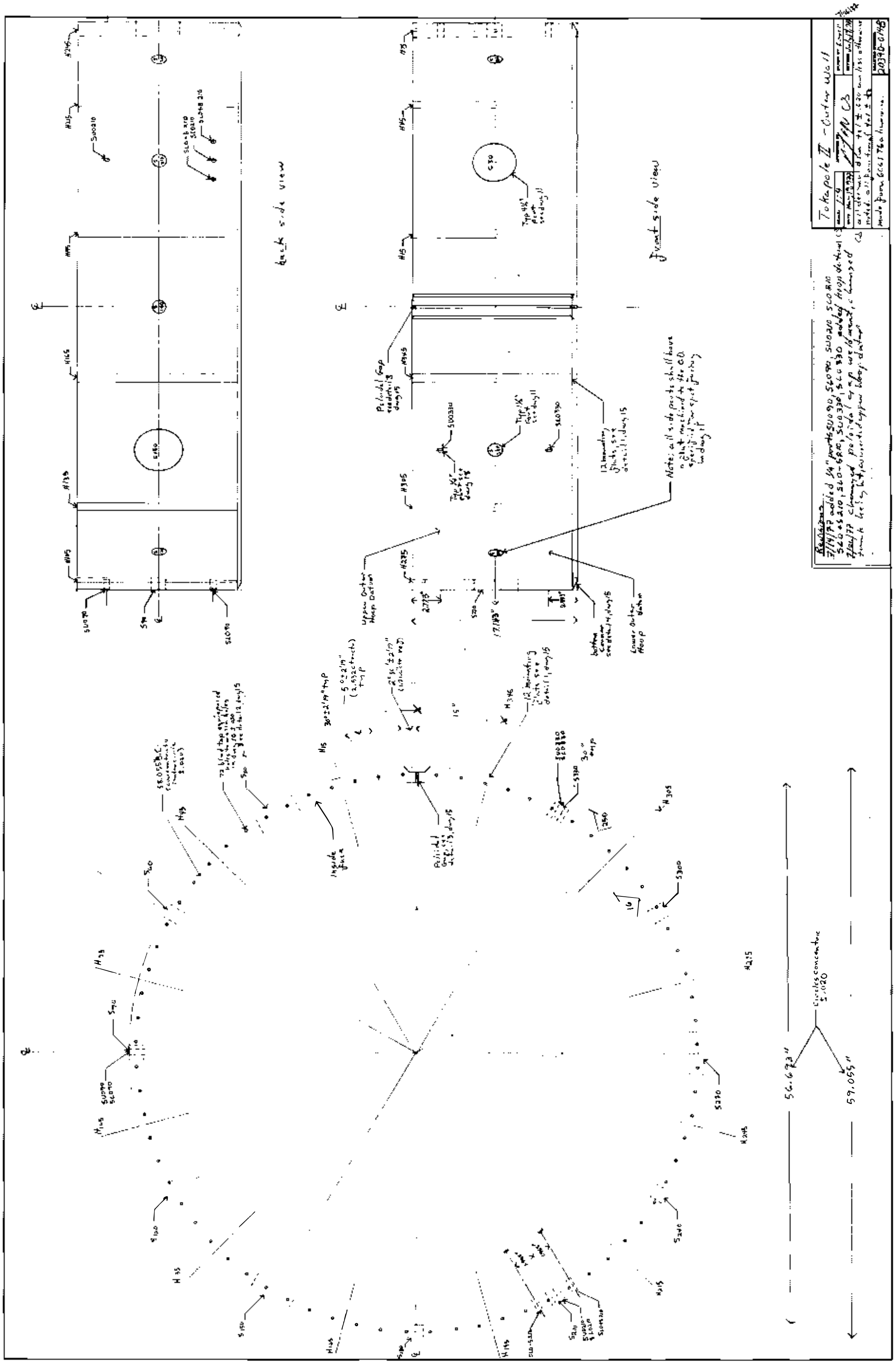
Tokapole II - Outer Wall
back side view
front side view
56.693"
59.055"

Figure 4

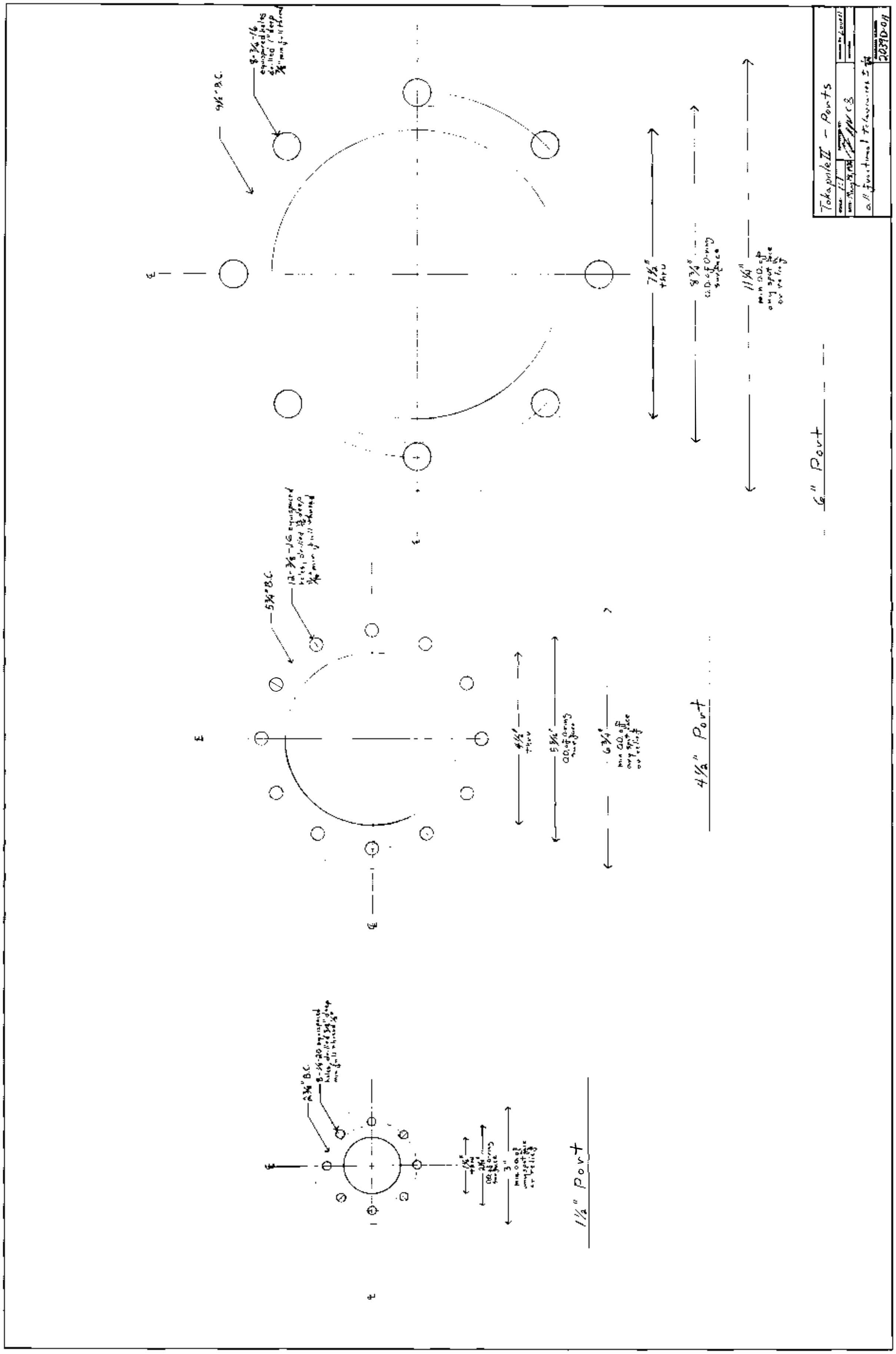

Tokapole II - Ports
6" Port
4½" Port
1½" Port
7½" thru
8¾" O.D. of O-ring surface
11¼" min O.D. of any spot face or relief
9¼" B.C.
5¾" B.C.
4½" thru
2¾" B.C.
3"

Figure 5

a vacuum material provided temperatures are kept below 200° C. and it is kept out of direct contact with the plasma. Fig. 6 shows the details of the insulated gaps.

All tolerances were specified as ±0.020" (0.5 mm) with particular attention paid to axisymmetry. The interior (vacuum) surface was machined to a high degree of smoothness (∿63 μinches) to reduce the effective surface area, but it was not polished for fear of trapping air pockets which would produce virtual leaks.

III. POLOIDAL FIELD SHAPE

Poloidal field configurations produced by fewer than three hoops are deemed unsatisfactory for toroidal ohmic heating because small toroidal currents are incapable of altering the field topology near the null. Very high order multipoles are unnecessarily complex, and so an octupole was chosen as a reasonable compromise. A configuration with four hoops makes the most effective use of the square cross section, and of course it is the configuration with which we have had the most experience.

Consideration was given to making hoops with multiturn imbedded conductors which could be driven independently of the ohmic heating transformer. The idea was rejected because of the difficulty of construction, because the optimum design would have put unacceptably large stresses in the hoops, and because careful programming of the currents would have been required to maintain a degenerate field null in the presence of plasma currents and field soak-in. The proportion of current flowing in the hoops and plasma can be adjusted over a wide range by varying the toroidal field, gas pressure, and preionization, and so the additional flexibility of having independently driven hoops was deemed unnecessary.

Program TORMESH (developed in 1963 by Dory and subsequently revised by Willig and most recently by Chu) was used to calculate poloidal magnetic flux plots and other quantities of interest for four hoops of arbitrary size and position within the square cross section previously decided upon. The program solves the equation,

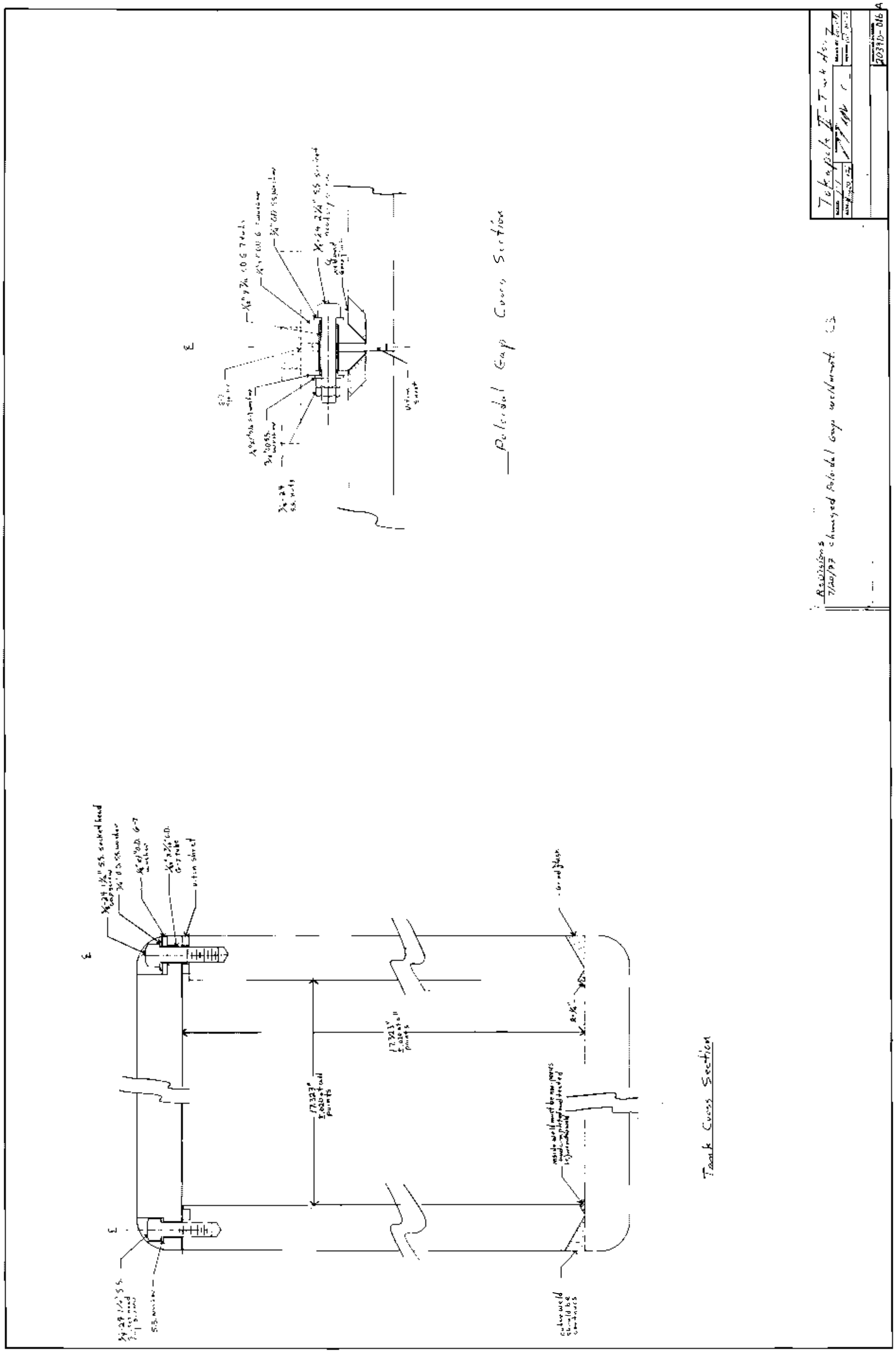

Figure 6

$$\frac{\partial^2\psi}{\partial R^2} - \frac{1}{R}\frac{\partial\psi}{\partial R} + \frac{\partial^2\psi}{\partial Z^2} = 0$$

with $\psi = 0$ at the hoops and $\psi = 10$ at the walls for cases in which the field is symmetric about the median plane. It also calculates contours of constant $|\vec{B}|$, currents in the hoops and walls, total inductance, position of the separatrix and ψ-critical (the outermost MHD stable flux surface), and the vertical component of the magnetic force on each hoop.

The design criteria for the flux plot were as follows:

1) A single degenerate octupole field null

2) The separatrix at $\psi \simeq 5.0$

3) ψ critical $\gtrsim 8.0$

4) Hoops as far from the minor axis as possible for reasonable stresses

5) Minimum required exposed hanger area

6) Insensitivity of null degeneracy to field soak-in.

After examining about a dozen cases, it was determined that the above conditions were most nearly met by a configuration in which all hoops have a minor diameter of 5 cm. and are placed in nearly symmetric places relative to the corners of the vacuum vessel. The slight asymmetry was necessary to provide a degenerate null. It was found that very small (~ 1 mm.) displacements of a hoop caused the nulls to separate by several cm., and so close tolerances in the original construction and some degree of adjustability were considered essential. The final dimensions decided upon were as follows:

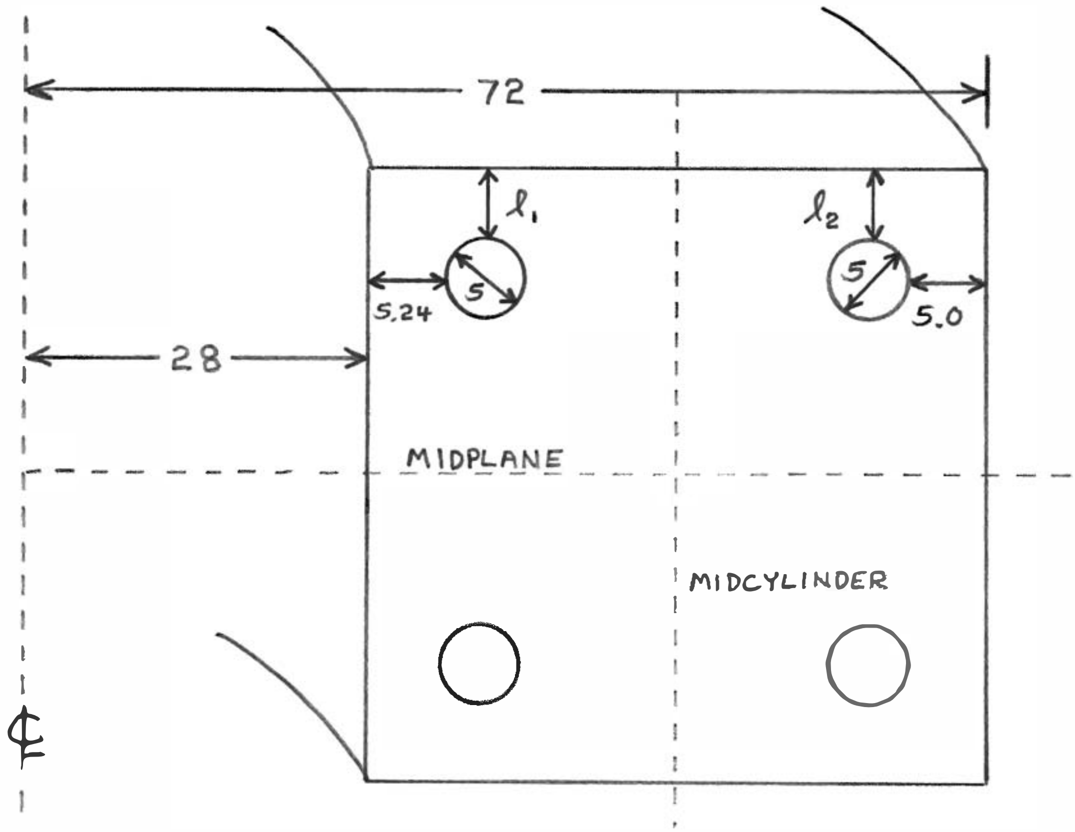

All dimensions are in cm., and the device is symmetric about the horizontal midplane. The nominal vertical hoop positions are ℓ_1 = 5.24 cm and ℓ_2 = 5.00 cm, and each hoop is vertically adjustable ±0.5 cm about its nominal position. The poloidal magnetic flux plot is shown in figure 7, and the contours of constant magnetic field (normalized to 1.0 at the outside wall midplane) are shown in figure 8. The field strength on the midplane and midcylinder are plotted in figure 9. The quantity $\oint \frac{d\ell}{B}$ is plotted as a function of ψ in figure 10. The other parameters for this configuration are given under the "Case 10" column of table III for a total flux of 0.15 webers which is about the sauration flux for the iron core with reverse biasing. Also shown in table III are the results of moving the hoops ±0.5 cm vertically in various combinations (Cases 12, 15, 16, and 17). Finally, Table III lists Case 11, which is a variation of Case 10 in which the walls have been recessed 1 cm and the hoops reduced in radius by 0.75 cm to simulate a reasonable amount of soak-in corresponding roughly to the peak of a 9.2 msec half sine wave poloidal field. The ratio of skin depths, 3:4, was chosen as appropriate for hoops made of a copper alloy with 1.13% chromium, called Ampcoloy 97, which has a yield strength of 43,000 psi at 0.5% elongation, and a conductivity of 78% IACS. For this

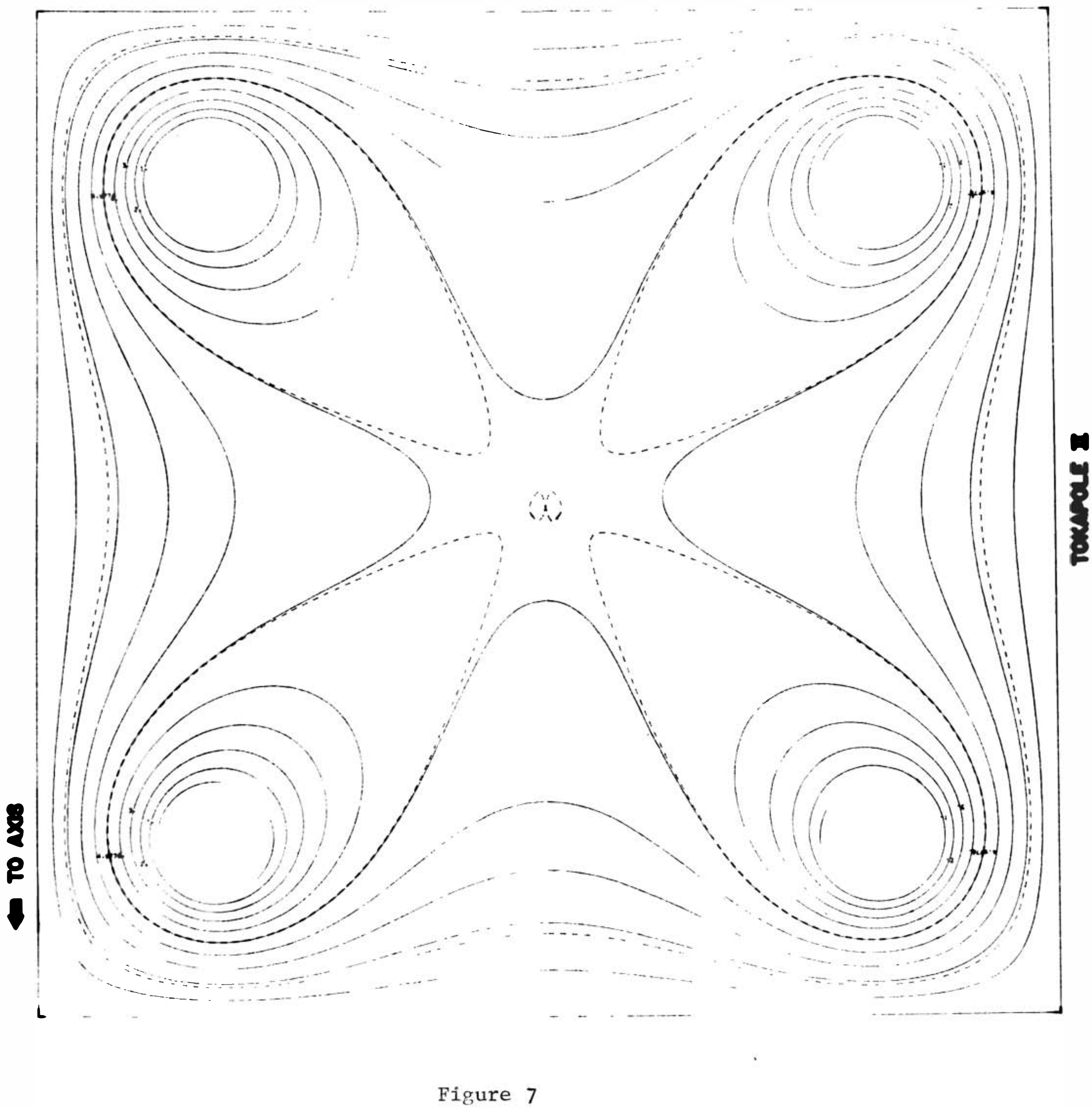

Figure 7

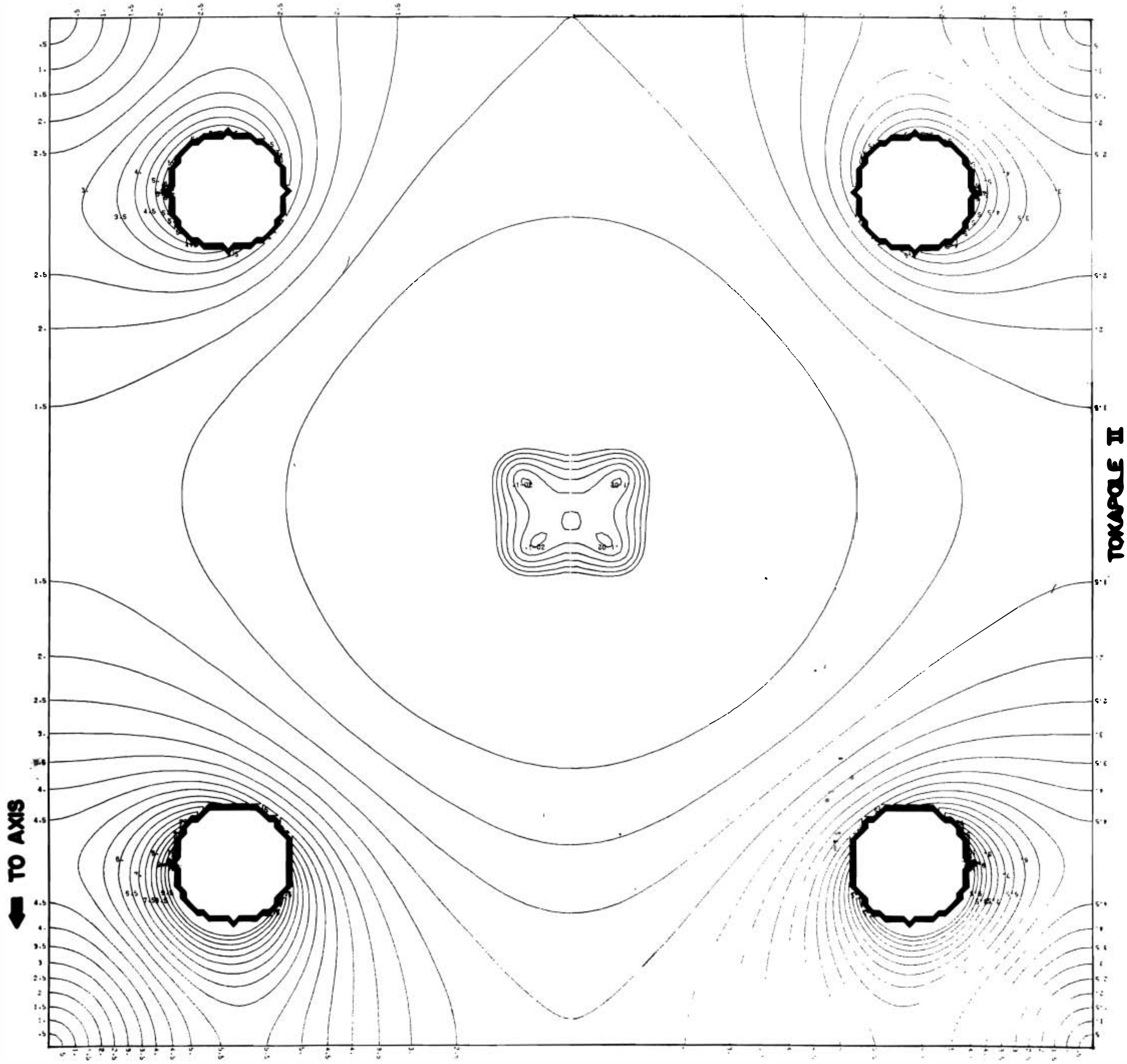

Figure 8

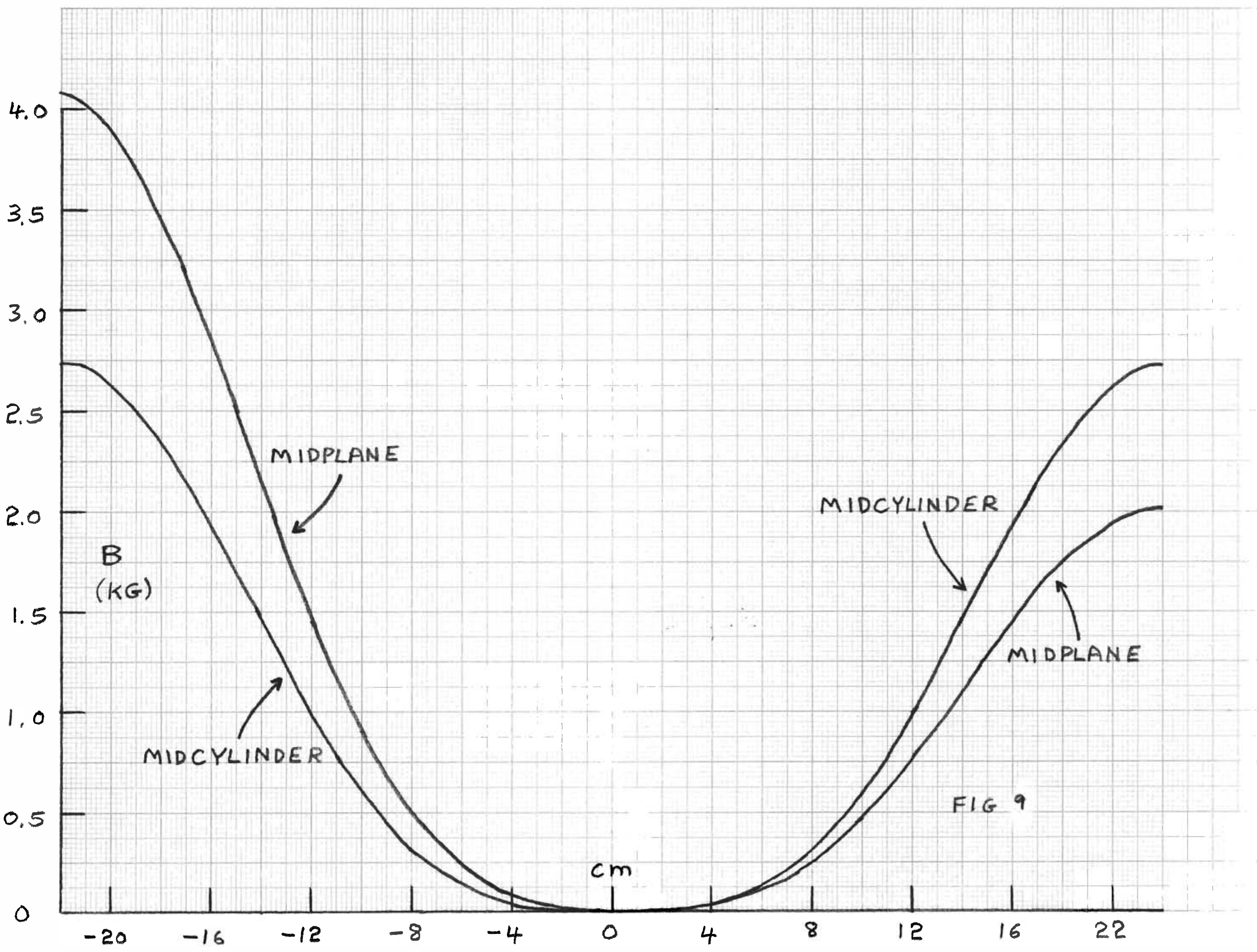
B
(kG)
4.0
3.5
3.0
2.5
2.0
1.5
1.0
0.5
0
-20
-16
-12
-8
-4
0
4
8
12
16
22
cm
MIDPLANE
MIDCYLINDER
MIDCYLINDER
MIDPLANE

FIG 9

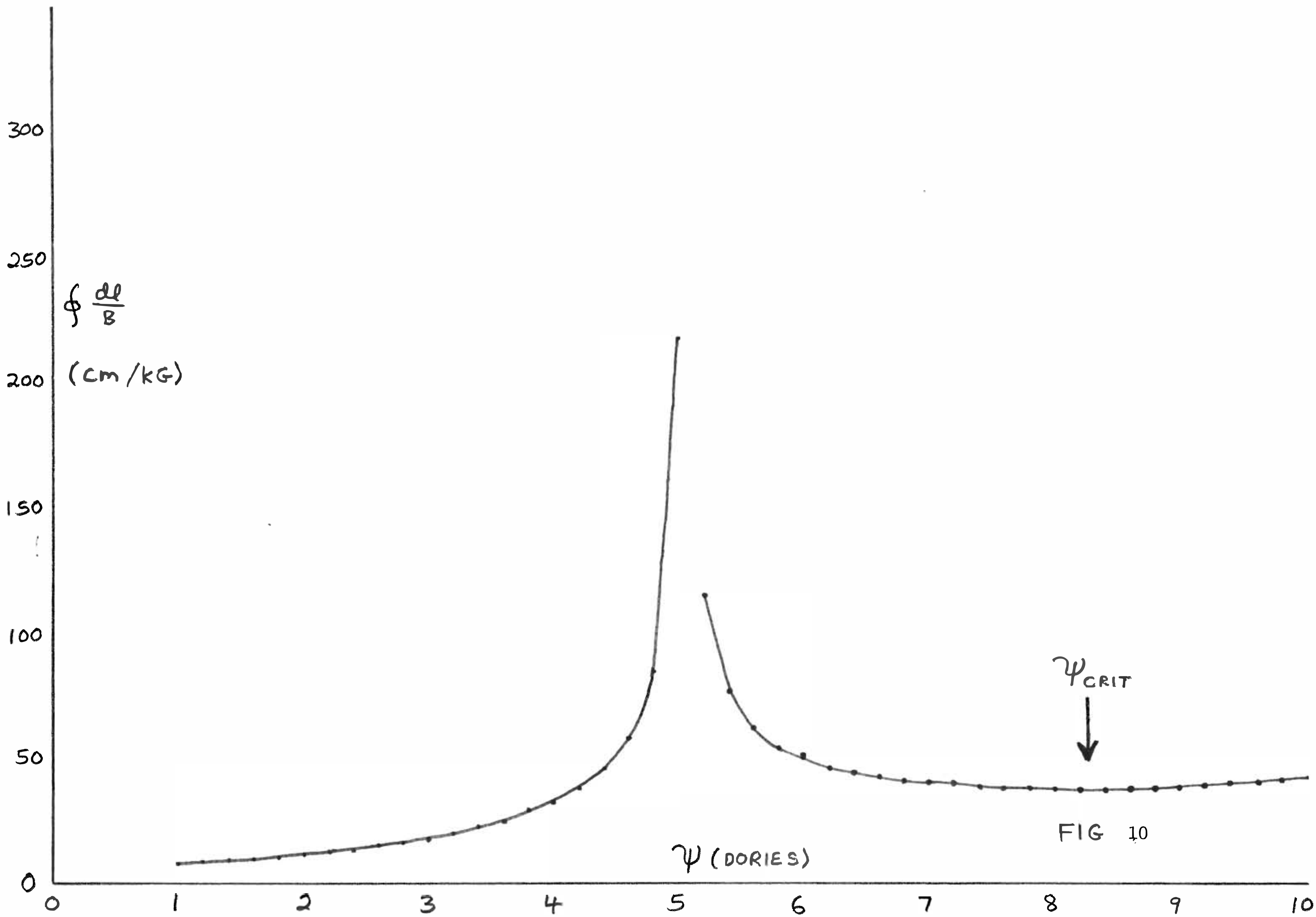

300
250
$\oint \frac{dl}{B}$
(cm/kG)
200
150
100
50
0
0 1 2 3 4 5 6 7 8 9 10
ψ (DORIES)
ψ_{CRIT}

FIG 10

TABLE III.

CHARACTERISTICS OF TOKAPOLE II IN OCTUPOLE MODE

QUANTITY	UNITS	CASE 10	CASE 12	CASE 15	CASE 18	CASE 19	CASE 11
ℓ_1	cm.	5.24	4.74	4.74	5.74	5.74	5.24
ℓ_2	cm.	5.00	5.50	4.50	5.50	4.50	5.00
Flux	webers	0.15	0.15	0.15	0.15	0.15	0.15
CURRENT							
Inner wall	kA	241	237	237	245	245	180
Outer wall	kA	115	117	113	117	114	85
Lid	kA	165	169	179	153	162	122
Inner hoop	kA	224	230	230	218	218	167
Outer hoop	kA	121	118	125	118	125	90
Total	kA	686	692	707	667	683	509
Inductance	μH	0.219	0.217	0.212	0.225	0.220	0.295
HOOP FORCE							
Inner	lb	20653	24368	24280	17668	17588	11111
Outer	lb	7194	6203	8385	6193	8416	6931
B - MP/OW	kG	2.01	2.12	1.90	2.13	1.92	1.69
MAX	kG	24.3	24.8	24.8	24.0	24.0	17.1
ψ-Separatrix	Dory	5.04	5.00	5.24	4.85	4.96	5.47
ψ-Critical	Dory	8.23	8.19	8.40	8.02	8.27	8.01
Field Energy	kJ	51.5	52.0	53.0	50.1	51.3	38.2
Null Error	cm	2.0	8.4	3.3	3.0	8.3	3.4
		DESIGN CASE	HOOPS DISPLACED VERTICALLY ±0.5 CM.				SOAK-IN CASE

case ~20% of the flux is lost in the hoops and ~12% is lost in the walls. More detailed soak-in calculations are under way using program SOAK (PLP 471).

In another series of runs, TORMESH was modified to study the effect of toroidal plasma currents on the poloidal flux plot by solving the equation

$$\frac{\partial^2\psi}{\partial R^2} - \frac{1}{R}\frac{\partial\psi}{\partial R} + \frac{\partial^2\psi}{\partial Z^2} = 2\pi\mu_\circ R j_T,$$

where the toroidal current density j_T was assumed to vary as 1/R over the entire cross-section (including the interior of the hoops). Table IV gives the results for various magnitudes of total toroidal plasma current for a hoop configuration as in Case 10. For these runs, the total flux was held constant (0.15 webers), and the separatrix was defined as the minimum value of ψ (in dories, where 1 dory is the total flux/10), along the horizontal midplane. For all these cases the plasma current flows toroidally in the same direction as the hoop currents, except for case 10F in which it flows opposite to the hoop currents.

The plasma current for all cases in Table IV is given to within ~15% by

$$I_p = \frac{10}{5.04}\,(I_{total} - \Phi/L)$$

where Φ is the total flux (which can be determined from the poloidal gap voltage V_{PG} by $\int V_{PG}dt$) and L is the unperturbed inductance (0.219 μhy). This relation is reasonably accurate even when the plasma current is greater than the hoop current and despite the fact that the current is distributed over the cross-section rather than being concentrated near the minor axis. Note also that the total hoop current decreases (or increases) by about 0.5A for every amp that flows in the plasma. These observations lend considerable credence to our method of measuring plasma current using the above equation. (See PLP 712)

TABLE IV.

CHARACTERISTICS OF TOKAPOLE II FOR VARIOUS PLASMA CURRENTS

QUANTITY	UNITS	CASE 10	CASE 10B	CASE 10C	CASE 10D	CASE 10E	CASE 10F
Flux	webers	0.15	0.15	0.15	0.15	0.15	0.15
CURRENT							
Plasma	kA	0	100	200	500	1000	-500
Inner wall	kA	241	262	283	345	449	147
Outer wall	kA	115	125	135	164	213	72
Lid	kA	165	178	192	232	300	102
Inner hoop	kA	224	211	198	160	133	287
Outer hoop	kA	121	114	106	83	72	160
Total	kA	686	743	801	973	1262	423
Inductance	μH	0.219	0.202	0.187	0.154	0.119	0.355
HOOP FORCE							
Inner	lb	20653	21969	22942	23409	17700	8547
Outer	lb	7194	7574	7769	7189	2622	2448
B - MP/OW	kG	2.01	2.52	3.03	4.57	7.12	0.54
MAX	kG	24.3	23.9	23.4	22.0	19.6	26.7
ψ-Separatrix	Dory	5.04	3.67	2.24	-1.83	-8.70	11.92
ψ-Critical	Dory	8.23	7.87	7.49	-	-	-
Field Energy	kJ	51.5	55.8	60.0	72.9	94.8	31.8
Null Position	cm	<2.0	6.9	9.7	14.4	16.0	17.4

IV. POLOIDAL FIELD PRIMARY AND CONTINUITY WINDINGS

An 80:1 turns ratio was chosen for the poloidal field because it was desired to get a slightly higher voltage/turn than was allowed by the 120:1 turns ratio of Tokapole I while keeping the poloidal field duration at least as long as the 10 msec half period of Tokapole I. It was also desired to have the capability of reducing the turns ratio to 40:1 to raise the secondary voltage to 125 volts with a period half as long. The poloidal field primary was to be wound in four sections, one on each leg of the iron core. In order to reduce any poloidal wall currents at the poloidal gap which would produce field errors, the number of turns on each leg was adjusted to be proportional to the current in the wall of the toroid nearest that leg as follows:

	CURRENT	TURNS REQUIRED	ROUNDED
inner wall	241.1 kA	28.12	27
outer wall	115.3 kA	13.45	13
top	164.7 kA	19.21	20
bottom	164.7 kA	19.21	20
total	685.8 kA	80.00	80

Since the number of turns must be an integer, the required number was rounded off. Twenty turns were put on the top and bottom despite the fact that 19 would have been a closer approximation because it simplified the task of allowing a 40 and an 80 turn connection. With the above arrangement, two connections are possible as shown below:

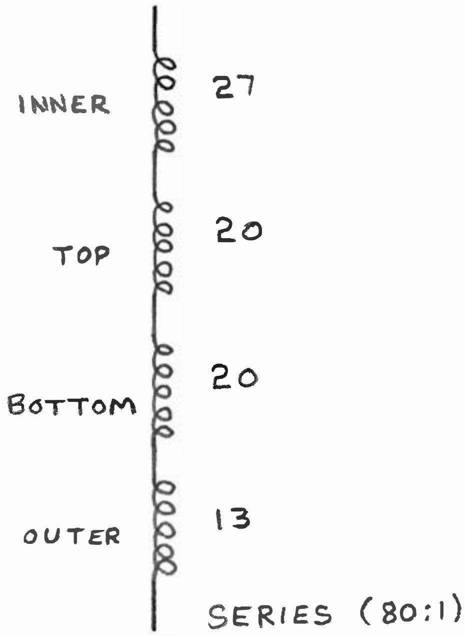

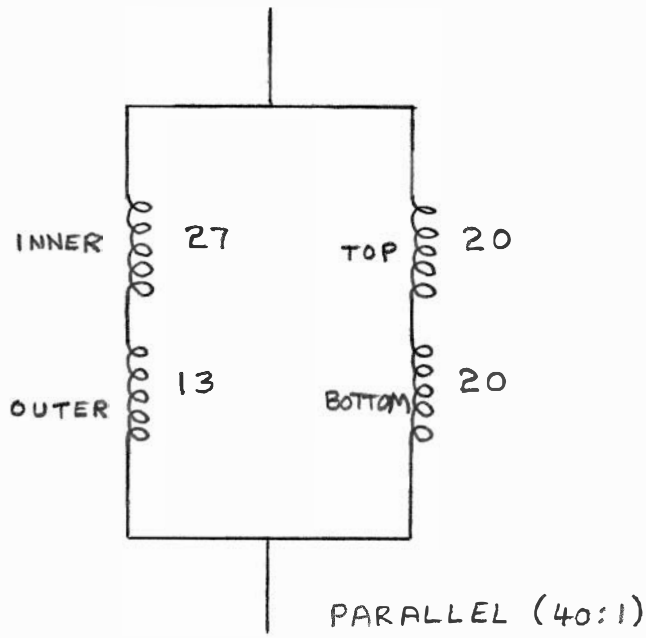

The error introduced by the rounding off amounts to about 4%.

In addition, the turns along each leg were wound with a density proportional to the surface current density at each point along the wall. The surface current density was determined from $\int B d\ell$ where $B(\ell)$ along each wall is given in figure11. The optimum placement of the primary turns is given in Table IV in terms of distance from the midplane or midcylinder. The closest winding spacing is about 1 cm./turn, and so for a single layer winding, the largest wire size that could be used is AWG Size 2. The wire chosen for the primary is stranded (133 strands), tinned copper, with silicone rubber insulation rated for 600V and 180° C., with a nominal OD of 0.455". Since this OD is slightly greater than the minimum turn spacing (0.390") it was necessary to deviate slightly from the placement indicated in table V. A sample of the wire survived a 1 hour bake in an oven at 260° C. with no ill effects.

Note that the winding distribution was optimized for the Case 10 octupole, and so it will not be quite correct if the hoops are displaced from their nominal positions, or if the field soaks into the hoops and walls, or if a toroidal current flows in the plasma. In the limit of $I_{plasma} >> I_{hoops}$ and distributed with a current density $j_T \propto 1/R$ over the whole cross section, the optimum turns ratio on the four legs of the transformer would be 30.8 : 18.6 : 18.6 : 12.0, which differs by ~12% from the chosen distribution in the worst case.

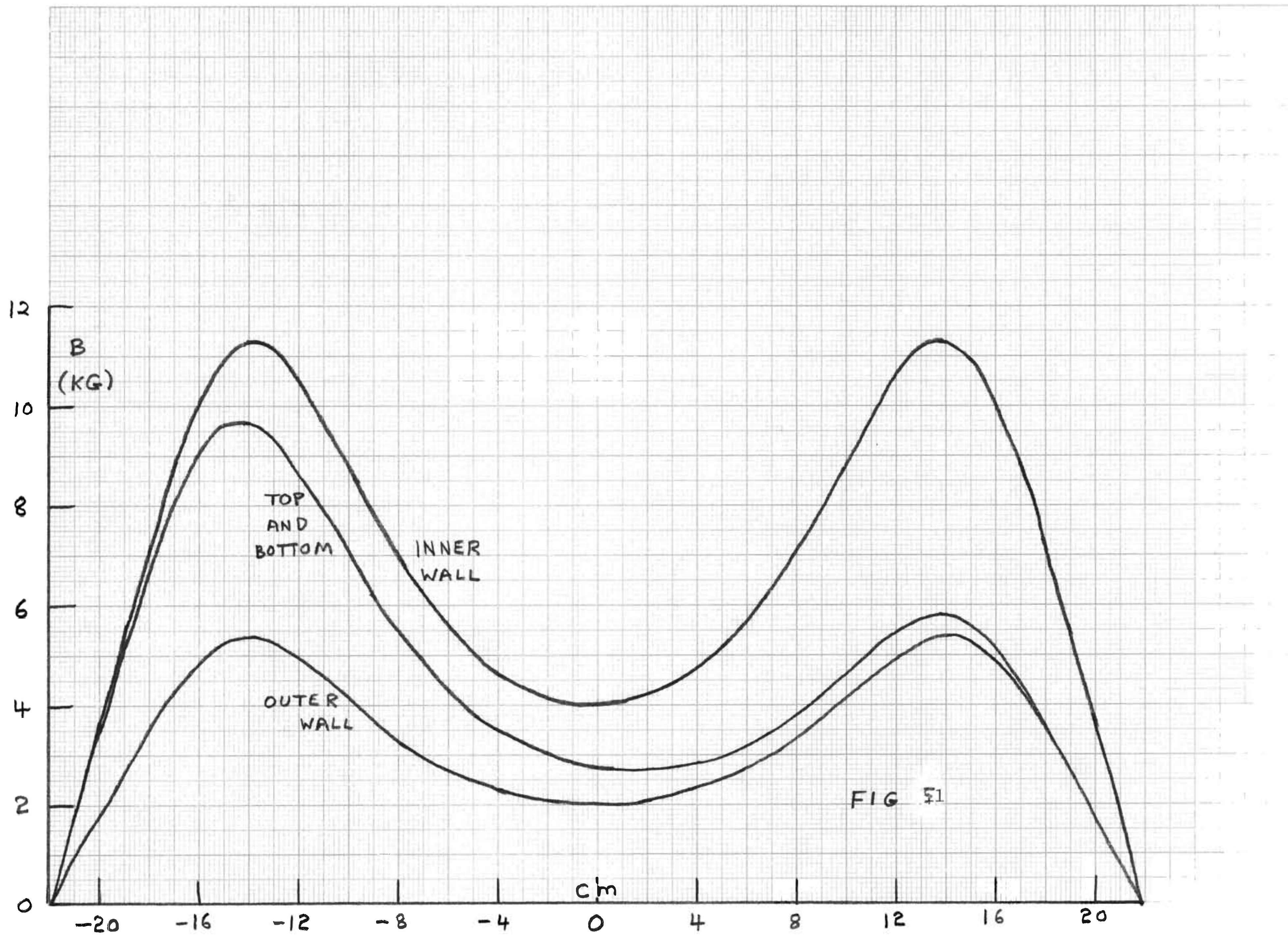
B (KG)
12
10
8
6
4
2
0
-20
-16
-12
-8
-4
0
4
8
12
16
20
cm
TOP AND BOTTOM
INNER WALL
OUTER WALL

FIG 51

TABLE V.

POSITION OF POLOIDAL FIELD WINDINGS

	INNER WALL		OUTER WALL		TOP AND BOTTOM	
	Optimum	Actual	Optimum	Actual	Optimum	Actual
1	-19.57 cm	-7.705"	-18.57 cm	-7.311"	-19.68 cm	-7.748"
2	-17.72	-7.032"	-15.75	-6.201"	-17.60	-6.929"
3	-16.39	-6.582"	-13.64	-5.376"	-16.33	-6.475"
4	-15.30	-6.132"	-11.47	-4.516"	-15.20	-6.025"
5	-14.28	-5.682"	- 8.83	-2.476"	-14.16	-5.575"
6	-13.29	-5.232"	- 5.12	-2.016"	-13.08	-5.125"
7	-12.27	-4.783"	0.00	0.00	-11.94	-4.675"
8	-11.19	-4.332"	5.12	2.016"	-10.69	-4.209"
9	-10.01	-3.882"	8.83	3.476"	- 9.22	-3.630"
10	- 8.64	-3.402"	11.47	4.516"	- 7.40	-2.913"
11	- 7.04	-2.772"	13.64	5.376"	- 4.95	-1.949"
12	- 5.10	-2.008"	15.75	6.201"	- 1.86	- .732"
13	- 2.70	-1.063"	18.57	7.311"	1.90	.748"
14	0.00	0.00"			5.56	2.189"
15	2.70	1.063"			8.52	3.354"
16	5.10	2.008"			10.80	4.252"
17	7.04	2.772"			12.71	5.004"
18	8.64	3.402"			14.49	5.705"
19	10.01	3.882"			16.41	6.461"
20	11.19	4.332"			19.12	7.528"
21	12.27	4.783"				
22	13.29	5.232"				
23	14.28	5.682"				
24	15.30	6.132"				
25	16.39	6.582"				
26	17.72	7.032"				
27	19.57	7.705"				

For continuity windings of reasonable thickness (say < 1/2"), the skin depth is greater than the thickness, and so they look like resistors rather than inductors. Since the same voltage appears everywhere along the poloidal gap, it is desirable to tailor the winding resistance per unit length along the gap inversely with the desired current density. To do this properly would have required a very fancy machining operation which would probably not be warranted by the improvement obtained. However, some attempt to match the wall currents was made by arranging the thickness of the four continuity windings in inverse proportion to the current in the respective wall, 115 : 165 : 165 : 224. A ratio of 4 : 3 : 3 : 2 satisfies this to within ~8% and so the continuity windings were designed using copper (for high conductivity) with a 1/4" thickness on the inner wall (the maximum thickness that could be easily bent to the desired radius), a 3/16" thickness on the top and bottom and a 1/8" thickness on the outer wall.

V. POLOIDAL FIELD ENERGY LOSSES

As shown previously, about 50 kJ of energy is required in the magnetic field for a total flux of 0.15 webers. In order to have some margin for losses, we will start by assuming a 90 kJ capacitor bank (30 - 240 μF, 5 kV capacitors). Ignoring soak-in, the 40 and 80 turn primary connections give half periods of 5 and 10 msec respectively. Extrapolating from the soak-in Case 11 of Table III the half periods are estimated to be about 5.5 and 12 msec, respectively. (The Case 11 flux plot is assumed to be correct at the peak of a 9.2 msec half sine wave.) The corresponding secondary inductances are estimated to be 0.264 and 0.318 μhy respectively. This is of course, an oversimplification, since the inductance actually rises during the pulse as the field soaks into the walls and hoops. The energy loss at peak field in the transmission line, primary, continuity windings, walls, and hoops will now be estimated for each of the two periods. The energy losses will be normalized against the energy stored in the field at the time of peak field.

A. Transmission line: The transmission line is assumed to consist of a twisted pair of 40' long #2 wires and is represented as a resistance of 0.013Ω in series with the primary LC circuit. The energy loss at peak field is given by

$$\Delta U = \int I^2 R dt = \int_0^{T/2} I_o^{\,2} R \sin^2 \omega t dt = \tfrac{1}{4} I_o^{\,2} RT,$$

where T is the half period and I_o is the peak primary current. But the stored energy is

$$U = \tfrac{1}{2} N^2 L I_o^{\,2}$$

where N is the turns ratio and L is the secondary inductance.

Then $$\frac{\Delta U}{U} = \frac{RT}{2N^2 L} = \begin{cases} 8.46\% \text{ for } T = 5.5 \text{ msec.} \\ 3.83\% \text{ for } T = 12 \text{ msec.} \end{cases}$$

B. Primary windings: The primary is assumed to consist of 2 - 192' lengths of #2 wire which are connected either in parallel or in series, depending on the desired field period. For the parallel connection, R = 0.0156Ω and for the series connection, R = 0.0624Ω. Then

$$\frac{\Delta U}{U} = \frac{RT}{2N^2L} = \begin{cases} 10.16\% \text{ for } T = 5.5 \text{ msec.} \\ 18.40\% \text{ for } T = 12 \text{ msec.} \end{cases}$$

C. Continuity windings: If the continuity windings are assumed to be thin compared with the skin depth and if the current is assumed to be distributed along the windings in the same way that it is distributed in the walls, then the energy lost in a winding is given by

$$\Delta U = \tfrac{1}{4} I_o^2 RTF$$

where F is a form factor given in terms of the wall current density $j_o(\ell)$ by

$$F = \frac{\ell \int j_o^2 d\ell}{(\int j_o d\ell)^2} = \frac{\ell \int B^2 d\ell}{(\int B d\ell)^2}$$

Integration of the $B(\ell)$ in figure 11 leads to the result that $F \cong 1.25$ for all continuity windings. Then

$$\frac{\Delta U}{U} = \frac{1.25 RT I_o^2}{2L I_o^2{}_{\text{total}}} = 0.625 \frac{RT\ I_o^2}{L I_o^2{}_{\text{total}}}$$

Assuming each continuity winding to be 141 cm long by 44 cm wide, the resistance for the three thicknesses are

$$R = \begin{cases} 8.6\mu\Omega \text{ for } 1/4'' \text{ thick} \\ 11.4\mu\Omega \text{ for } 3/16'' \text{ thick} \\ 17.2\mu\Omega \text{ for } 1/8'' \text{ thick} \end{cases}$$

The corresponding values of $\Delta U/U$ are:

	5.5 msec	12 msec
inner winding (1/4")	1.38%	2.50%
lid winding (3/16")	0.86%	1.56%
outer winding (1/8")	0.63%	1.15%

D. Walls: The energy losses in the walls are calculated the same way as in the continuity windings except the lengths are different and the current is assumed to flow in a thickness equal to a skin depth. The skin depth is taken as 1.03 cm for the 5.5 msec pulse and 1.52 cm for the 12 msec pulse. The resulting values for $\Delta U/U$ are given by:

	5.5 msec	12 msec
inner wall	1.06%	1.30%
lid	0.89%	1.09%
outer wall	0.63%	0.77%

E. Hoops: The energy losses in the hoops are calculated in a fashion similar to that used for the walls. The ac resistance of the hoops was taken as 20.61 $\mu\Omega$/meter at 90.9 Hz (5.5 msec half-period) and 14.92 $\mu\Omega$/meter at 41.7 Hz (12 msec half period) and the form factor F was taken as 1.06. Then the relative energy loss in each hoop is:

	5.5 msec	12 msec
inner hoop	5.45%	7.14%
outer hoop	2.87%	3.76%

The energy losses in each component of the system are summarized in table VI. The result is that, of the 90 kJ in the bank, about 60 kJ ends up stored in field in the machine, which is a comfortable margin above the ~50 kJ required for a flux of 0.15 webers. Other losses such as in the ignitron, iron core, and in contact resistance at the various electrical joints and energy stored in the core and in leakage fields may use up most of the difference.

TABLE VI.

SUMMARY OF POLOIDAL FIELD ENERGY LOSSES

	5.5 msec		12 msec	
	ΔU/U (%)	ΔU(kJ)	ΔU/U (%)	ΔU(kJ)
transmission line	8.46	5.34	3.83	2.22
primary	10.16	6.42	18.40	10.68
inner continuity winding	1.38	0.87	2.50	1.45
top continuity winding	0.86	0.54	1.56	0.91
bottom continuity winding	0.86	0.54	1.56	0.91
outer continuity winding	0.63	0.40	1.15	0.67
inner wall	1.06	0.67	1.30	0.75
top wall	0.89	0.56	1.09	0.63
bottom wall	0.89	0.56	1.09	0.63
outer wall	0.63	0.40	0.77	0.45
UI hoop	5.45	3.44	7.14	4.14
LI hoop	5.45	3.44	7.14	4.14
UO hoop	2.87	1.81	3.76	2.18
LO hoop	2.87	1.81	3.76	2.18
total loss	42.46	26.82	55.05	31.95
energy available	142.46	90.00	155.05	90.00
energy stored in field	100.00	63.18	100.00	58.05

For some purposes it is useful to represent the primary circuit as a series RLC, realizing that both L and R actually change somewhat during the pulse. The parameters for such a representation are given below.

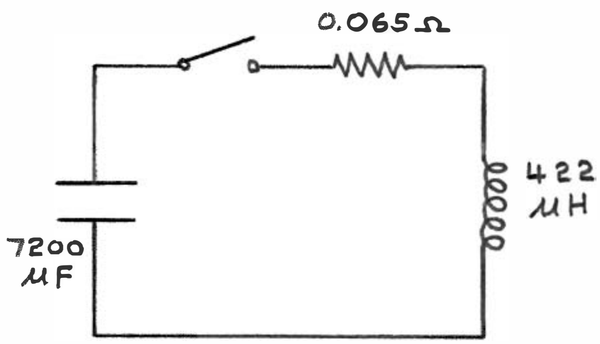

5.5 msec half-period

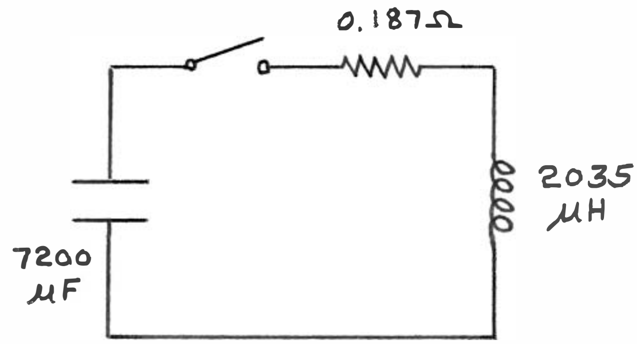

12 msec half-period

The L/R time for the two cases are 6.5 and 10.9 msec, and so we would not expect to gain a great deal by use of a passive crowbar. A power crowbar would need 1.1 or 1.6 kV respectively at peak field to overcome the losses for the two winding configurations. The electrical Q for the two cases are 3.73 and 2.84. The reverse swing of the voltage should leave the capacitors charged to 3.27 kV and 2.85 kV respectively for an initial charge of -5 kV.

In order to maintain a poloidal gap voltage of say 10 volts (∿5 volts/turn at the separatrix), a power crowbar of 760 volts would be required with the 40:1 turns ratio, neglecting energy dissipated by ohmic heating of the plasma. For an RC decay time of 20 msec, a capacitance of ∿300,000 μF (∿90 kJ) would be required. Of course the iron core will saturate after a time t given by $\int_0^t V_{PG}\, dt \cong 0.15$ volt-sec.

The most severe heating problem is expected to occur at the inner hoop. Assuming $\Delta U = 3.44$ kJ/pulse/hoop and no heat losses, the temperature rise is given by

$$\Delta T = \frac{\Delta U}{MC}$$

where M = hoop mass = 39.14 kg

and C = heat capacity ≅ 389 J/kg/°C.

For the above numbers, we predict $\sim$0.226° C. rise per pulse. After ten hours of operation at 1 pulse/minute at full amplitude, the inner hoops would be at $\sim$150° C., if we ignore heat loss by radiation and by conduction along the hangers. Such a rise is acceptable, but not so small as to relieve us of all concern.

Complete data on the performance of metals at high temperature are not available. However, since all three important structural metals in Tokapole II (6061-T6 aluminum, Berylco 25 HT beryllium copper, and Ampcoloy 97 chromium copper) are strengthened by precipitation heat treatment, it seems logical that a general idea of high temperature performance can be inferred from the partial data available for each.

Mark's *Standard Handbook for Mechanical Engineers* (7th Ed., McGraw-Hill, 1967, pg. 690) lists 6061-T6 aluminum as having a tensile strength of 45 Kpsi at 75° F. (24° C.); at 300° F. (149° C.) it drops to 31 Kpsi, about 31%. At 400° F. (205° C.) it further drops to 19 Kpsi (58%) and at 500° F. (260° C.) it drops to 7.5 Kpsi (83%). Now the usual precipitation heat treating temperature for 6061-T6 is (*ibid.* Mark's, pg. 6-91) 315-325° F. (157-163° C.) so it is apparent that severe loss of strength occurs around that temperature. Heat treating temperature for Berylco 25 is 600° F. (316° C.) (PLP 137) and for Ampcoloy 97 (*Standards Handbook Alloy Data 12*, Copper Development Assoc. 1973), it is 800-930° F. (425-500° C.).

Graphs in PLP 137 (Fig. 4) provided by the Beryllium Corporation, show that permanent reduction in strength is not achieved for Berylco 25 until the precipitation heat treating temperature is reached. At that point strength deteriorates rather sharply with additional time and temperature. The solution heat treatment temperatures are somewhat immaterial since they require a rapid quench to return the material to the annealed state. For the sake of completeness they are: 6061-T6, 960-980° F.; Berylco 25, 1425-1475° F.; and Ampcoloy 97, 1800-1850° F.

The final hoops as delivered from Ampco were only guaranteed at a tensile strength of 60 Kpsi. Since we calculated stresses of around 50 Kpsi (pg. 24-25), a >20% reduction in strength could be disastrous. On the admittedly wild supposition that Ampcoloy 97 behaves like 6061-T6 and that up to the heat treating temperature the loss of strength is linear with temperature, the danger point might be about 500° F. (260° C.). For the hangers, the critical temperature is probably around 300° F. (149° C.).

VI. HOOP AND HANGER DESIGN

The hoops are driven by the pressure of the magnetic field toward the minor axis as shown below.

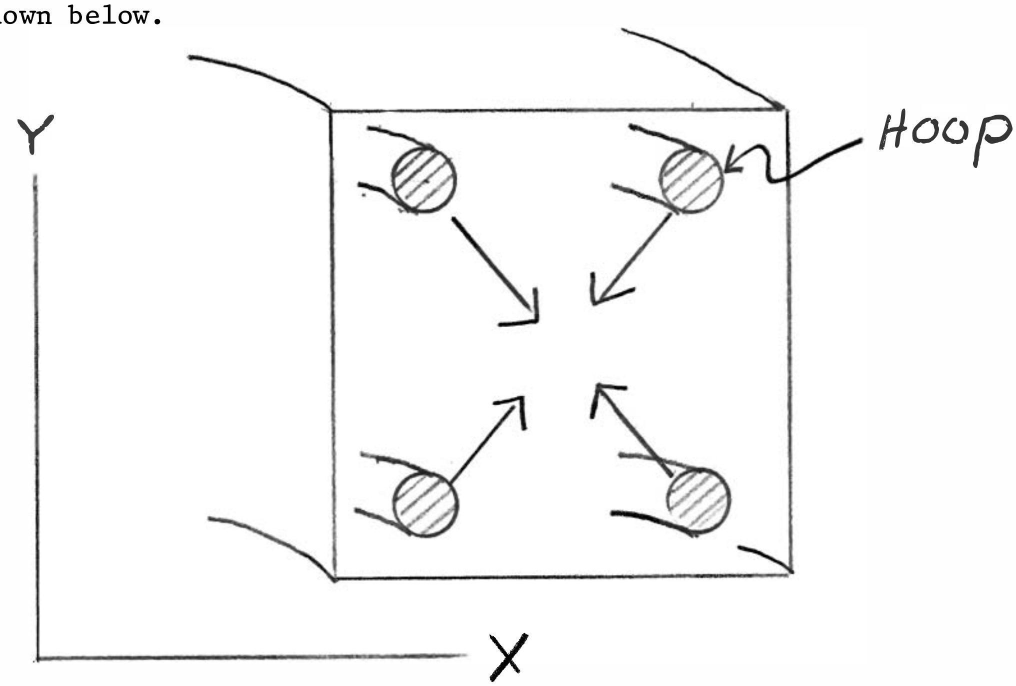

This force can be resolved into two components: an X axis force that is balanced by the hoops themselves (inner hoops in tension, outer hoops in compression) and a Y axis force that must be balanced by the hangers. Soak-in flux plot calculations show that the largest forces occur during the 5.5 msec. pulse and that the net Y axis magnitude is 12,496 lbs. on the inner hoops, and 7,933 lbs. on the outer hoops.

This force results in energy being stored in the springiness of the hoops and hangers. This energy is released in a rebounding of the hoop-hanger system. The forces on this system can exceed the applied force by as much as a factor of 1.7 (Morin, PLP 30), depending on the ratio of the frequency of mechanical resonance to the frequency of the applied force. Rather than attempting to calculate all the frequencies of all the modes of mechanical resonance for the system, a factor of 1.7 was uniformly applied. Hopefully, this results in a reasonably conservative safety factor in the design.

The hangers may fail either in tension or by buckling on the rebound. It can be shown (Morin, PLP 30) that the greatest stress results from yield buckling, a mode where the hanger is subject to simultaneous compression and bending due to an offset in the applied force.

$$F_y = \frac{\frac{\pi d^2}{4}\sigma}{1 + \frac{6\varepsilon}{d}}$$

F_y = force at yield buckling
d = diameter of hanger
σ = yield stress of material
ε = offset of force

F_y in the above equation must be kept less than the actual force on the hanger. The actual force is calculated by dividing the net force on a hoop by three, since there are three hangers per hoop, and multiplying by 1.7 for resonance. For the 5.5 msec. case, this results in a force of 7,081 lbs. for each inner hanger and 4,495 lbs. for each outer hanger. ε was set at 0.02" since this is the machine tolerance and σ was 165,000 psi, the yield of Berylco 25 HT, the hanger material. This is a beryllium-copper alloy that is precipitation-hardened (2 hr @ 600° F.) after machining.

The results of calculations using this formula and allowing an additional 1.1 safety margin to take into account stress raisers, was a diameter of 0.295" for the inner hangers and 0.245" for the outer hangers. These dimensions give a total hanger area exposed to the plasma of 133 cm^2, which is slightly smaller than the 144 cm^2 in the old octupole.

The hangers must be mounted in the hoops by some method. The criteria for this method were (1) strength, (2) minimum projection into the plasma, and (3) minimum area in the hoop to minimize field errors and power loss. After considering many schemes, the best seemed to be threading the hangers into the hoop with a pressed-in pin inserted to keep them from loosening. In addition, the area around the first few threads on the hoop was relieved to allow those threads to stretch and more evenly distribute the force. This scheme evolved during testing of the latest hangers in the little octupole and worked nicely to avoid a large stress raiser at the junction of the threaded hanger and the holding nut. R. E. Peterson, in an article in *Machine Design* (March 1951) confirms that a large stress raiser exists in the end thread of a tensile loaded threaded member. The design appears below.

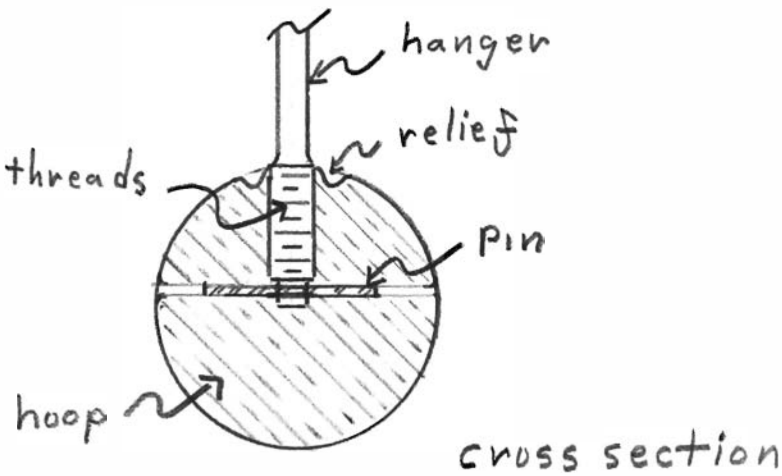

The thread strength calculations were done by the method of the "Machinery's Handbook" (Industrial Press, 1976, 20th Ed.), p. 1169:

$$F = \sigma A_t$$

F = force at yield

σ = tensile yield of material

At = tensile area from thread tables

The minimum engagement length is given by:

$$L_e = \frac{2A_t}{\pi Kn_{max}\left(\frac{1}{2} + \frac{n(Es_{min} - Kn_{max})}{\tan 60°}\right)}$$

L_e = length of engagement

Kn = minor diameter of internal thread

Es = pitch diameter of external thread

n = threads per inch

where the maximum and minimum values are taken from tables describing the class of fit.

The hoop and hanger will be made from different materials, so a correction must be made to account for the different tensile strengths.

$$Q = \text{length needed} = JLe$$

$$J = \frac{As\sigma_{ext}}{A_n\sigma_{int}}$$

where σ_{ext} = tensile strength of material of external thread

σ_{int} = tensile strength of material of internal thread

E_n = pitch diameter of internal thread

D_s = major diameter of external thread

$$An = \text{shear area of internal thread} = \pi nLeDs_{min}\left[\frac{n}{2} + \frac{(Ds_{min} - En_{max})}{\tan 60°}\right]$$

$$As = \text{shear area of external thread} = \pi nLeKn_{max}\left[\frac{n}{2} + \frac{Es_{min} - Kn_{max}}{\tan 60°}\right]$$

Using 120,000 psi as σ for Berylco 25 to remain in the Hookian region of the stress-strain curve, the minimum tensile areas are 0.059 in^2 for the inner hangers and 0.038 in.^{2} for the outer hangers. In order to minimize stress raisers as well as to insure sufficient thread strength, the threads chosen are nearly twice as strong. A 7/16-28, class 3 thread (At = .127 in.^{2}) was chosen for the inner hangers and a 5/16-28, class 3 thread (At = 0.061 in.^{2} for the outer hangers. Using 120,000 psi for σ_{ext} (Berylco 25 hanger) and 65,000 psi for σ_{int} (Ampcoloy 97, a chromium-copper alloy hoop) results in Q = 0.487" for the inner hangers and Q = 0.325" for the outer hangers. The actual thread engagement in both cases will be about 3/4", so we have a good safety margin.

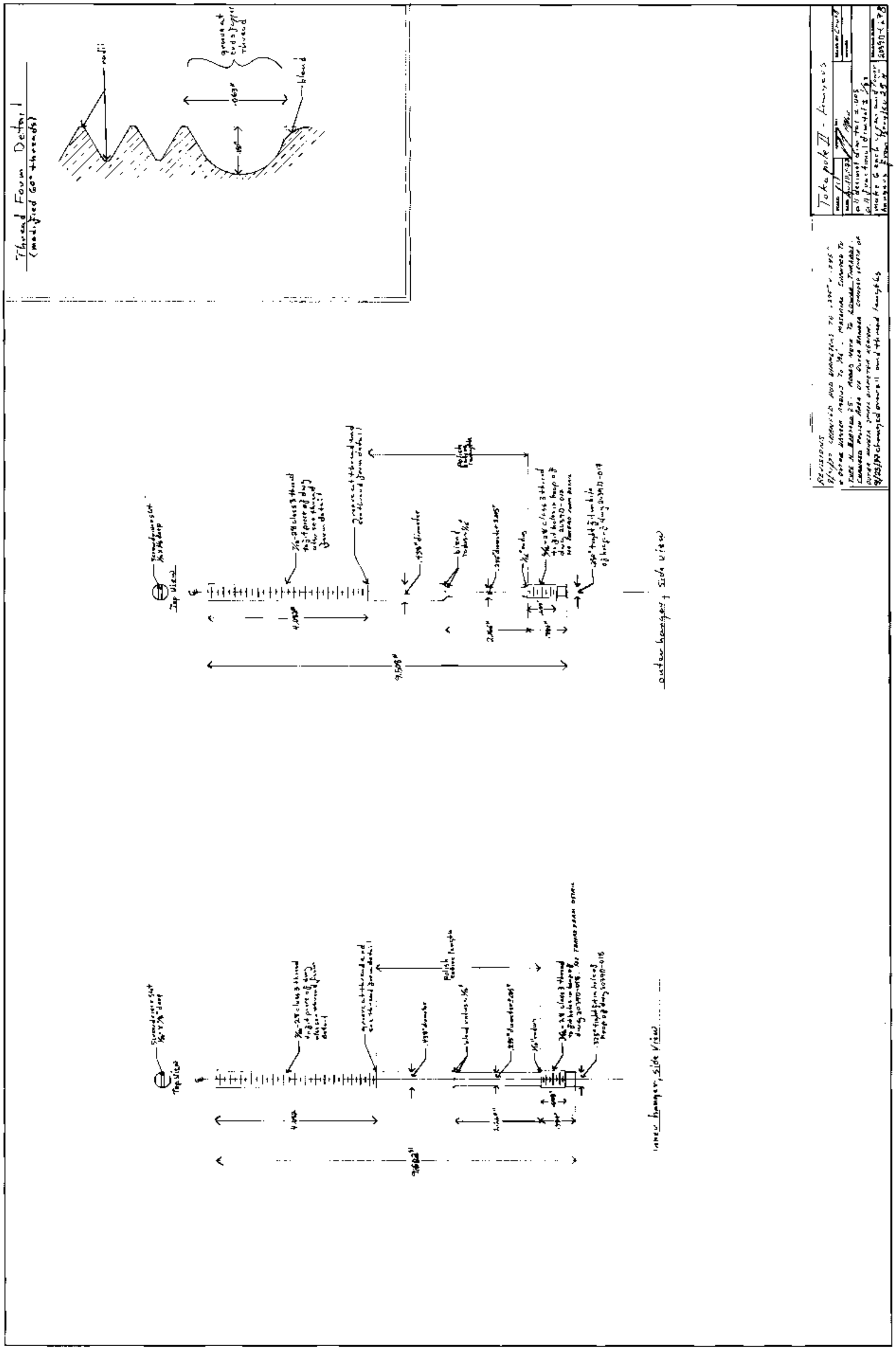
Thread Form Detail
(modified 60° threads)
Top View
outer hanger, side view
inner hanger, side view
Revisions

Figure 12

The top adjusting thread of both hangers was maintained to a 7/16" dia. like the previous octupole hangers, but the threading was increased to 28 threads per inch for finer adjustment of hoop position. The detailed hanger design is shown in fig. 12.

Since the hoops are supported in only three places, the force on them is converted to strain energy in shear, bending, and torque. The relative magnitudes of these energies depend on the nature of the supports and the shape of the hoop. For example, if the supports resist rolling and the chord between supports is a large fraction of the major hoop diameter, considerable energy is stored in torque. Problems of this sort can be solved using Castigliano's theorems (strain energy and least work). Roark and Young in "Formulas for Stress and Strain" (McGraw-Hill 1975, 5th ed.) give solutions to many similar cases, and it was their methods that were used.

In order to use these procedures, one must select a description of the method of support. Our hangers don't seem to fit neatly into any of the categories. However, for closed rings, uniformly loaded, Roark (p. 281) suggests a combination of simple support with slope guidance. This is a condition of zero torque and requires the hoop to be free to roll at the supports. Of course our hangers resist roll, but later calculations of the roll angle ψ_a show it to be small, resulting in a small force on hanger and hoop, justifying our assumption.

Roark's method requires the calculation of many constants and the subsequent use of them in rather complex formulae. Rather than reproduce what is available by referring to his book, the values calculated for those constants and the condensed formulae obtained by their application are listed below.

The second moment of area I' (commonly called the moment of inertia) was calculated for the hoop section with the hanger hole in it by the standard method of subtracting the moment of the hole from the moment of the hoop area. A correction was also

applied for the extreme fiber distance, c. The whole section, second moment I,
was used in the calculation of the original constants.

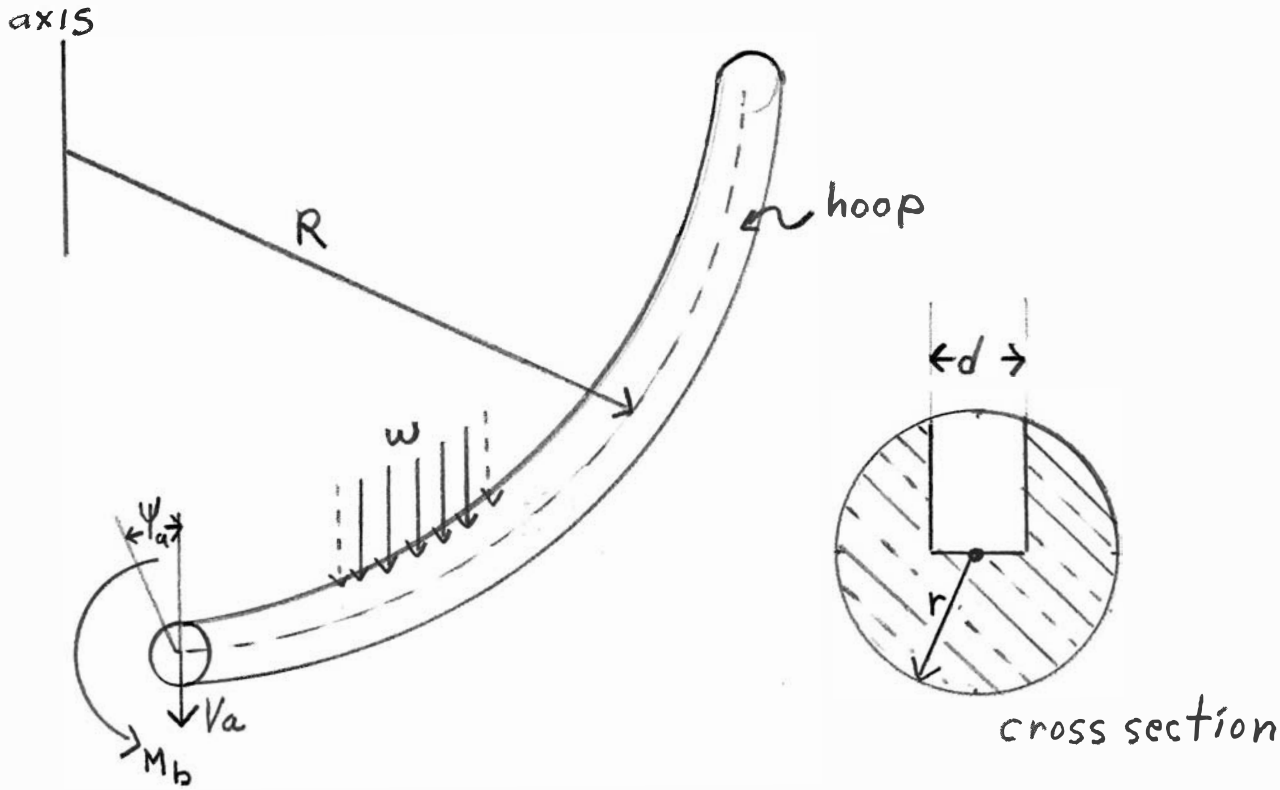

CONSTANTS

C_1	= .207	C_9	= −2.085	I (whole section)	= .736
C_2	= 2.085	Ca_{13}	= .475	K (whole section)	= 1.473
C_3	= .636	Ca_{16}	= .636	G (Ampcoly 97)	= 7.2×10^6
C_4	= 1.063	Ca_{19}	= 1.293	E (Ampcoly 97)	= 1.7×10^7
C_5	= 1.977	ϕ	= 2.094		
C_6	= .207	θ	= 0		
C_7	= 1.977	β	= 1.18		
C_8	= 1.219				

$$w = \frac{W}{2\pi R} \qquad W = \text{total load on hoop}$$

$$V_a \text{ (shear moment)} = 1.08\ wR$$

$$M_a \text{ (bending moment)} = -\ .452\ wR^2$$

$$\sigma_{bending} = \frac{M_a}{I'/c}$$

$$I' = \frac{\pi r^4}{4} - \frac{dr^3}{3} \qquad r = .984'' \qquad d_{inner} = .4375'',\ I'_{inner} = .585$$

$$d_{outer} = .3125'',\ I'_{outer} = .597$$

$$c = \tfrac{1}{2}\sqrt{4r^2 - d^2} \qquad c_{inner} = .943$$

$$c_{outer} = .959$$

$$\frac{I'}{c} = .591 \text{ inner, } .623 \text{ outer}$$

$$\psi_a \text{ (deflection angle)} = -\ .0787\ \frac{wR^3}{EI'}$$

$$\sigma_{tension} = \frac{W}{\pi r^2 - rd}$$

$$\tau_{shear} = \frac{V_a}{\pi r^2 - rd}$$

The holes for mounting the hangers create stress raisers in the hoop, and so it is important to estimate the increased magnitude of the stress. Roark gives theoretical formulae, but similar data are available in graphic form in both "The Handbook of Stress and Strength" (Lipson and Juvinall, Macmillan, 1963) and a series of articles in *Machine Design* (February through July, 1951, by R. E. Peterson). Review of the literature indicates that precise answers are difficult to come by, due to variations in materials, rate of strain, etc. Consequently the graphical method was chosen as being the easiest.

In order to utilize these methods, the hole in the hoop was assumed to continue all the way through the hoop and to be empty. Clearly this is a worst-case assumption, since strength is gained both on the undrilled section of the hoop and the hanger material in the hole.

Basically, the method consists of calculating a nominal stress based on the effective cross-section and then consulting the appropriate table to find the theoretical stress concentration factor K_t based on the ratio of the hole size to hoop minor diameter. K_t is only the appropriate factor for completely non-ductile materials and must be modified by an index of sensitivity, q (*Machinery's Handbook*, p. 361) to arrive at the actual stress concentration K. A q of .2 was chosen as fairly conservative. The Ks for the inner hoops were used for the outer hoops also. While they would be slightly smaller for the outer hoop, the accuracy of the calculation isn't changed significantly since the Ks are approximations to begin with.

resonance factor Kr = 1.7

bending stress concentration factor K_b = 1.17

tensile stress concentration factor K_e = 1.23

shear stress concentration factor K_s = 1.20

$$K = 1 + q(k_t - 1)$$

$$\hat{\sigma} = K\sigma$$

Since the force vector acts at about a 45° diagonal in the machine, another load (tensile in the inner hoop, compressive in the outer) equal to the load in the plane of the hangers is assumed to exist. The stress due to this load and the stress due to the shear moment must be combined with the bending stress to get the actual stress on the material. Roark gives a formula for biaxial stress plus shear. All stresses acting along the same axis were presumed to add:

$$\tau_c \text{ (combined shear) } = \sqrt{\frac{(\hat{\sigma}_b + \hat{\sigma}_t)^2}{4} + \tau^2}$$

$$\sigma_c \text{ (combined stress) } = \frac{\hat{\sigma}_b + \hat{\sigma}_t}{2} + \tau_c$$

The results of these calculations are as follows:

OUTER HOOP R = 25.394"

HALF PERIOD	*5.5 msec.*	*12 msec.*
w	49.7 lb./in.	39.5 lb./in.
V_a	1363	1083
M_a	-14,490	-11,510
σ_b	-22,080 psi	-17,550 psi
× Kr	1.7	1.7
× Kb	1.17	1.17
$\hat{\sigma}_b$	-43,920 psi	-34,910 psi
ψ_a	-5.9×10^{-3}	-4.7×10^{-3}
σ_t	2,901 psi	2,308 psi
× Kr	1.7	1.7
× Ke	1.23	1.23
$\hat{\sigma}_t$	6,066 psi	4,827 psi
τ	499 psi	396 psi
× Kr	1.7	1.7
× Ks	1.2	1.2
$\hat{\tau}$	1,017 psi	808 psi
τ_c	25,010 psi	19,880 psi
σ_c	50,010 psi	39,850 psi

INNER HOOP R = 14.070"

HALF PERIOD	*5.5 msec.*	*12 msec.*
w	141.4 lb./in.	115.3 lb./in.
V_a	2,148	1,752
M_a	-12,650	-10,310
σ_b	-20,310 psi	-16,550 psi

HALF PERIOD	*5.5 msec.*	*12 msec.*
$\times$ Kr	1.7	1.7
$\times$ Kb	1.17	1.17
$\hat{\sigma}_b$	-40,390 psi	-32,910 psi
ψ_a	-3.1×10^{-3}	-2.5×10^{-3}
$\hat{\sigma}_t$	4,785 psi	3,903 psi
$\times$ Kr	1.7	1.7
$\times$ Ke	1.23	1.23
$\hat{\sigma}_t$	10,010 psi	8,160 psi
τ	823 psi	671
$\times$ Kr	1.7	1.7
$\times$ Ks	1.2	1.2
$\hat{\tau}$	1,678 psi	1,369 psi
τ_c	25,260 psi	20,580 psi
σ_c	50,460 psi	41,120 psi

Therefore we find ourselves slightly above the 43,000 psi yield of Ampcoloy 97. Care will have to be taken to insure that the hangers are snugly mounted in their holes to prevent any pounding, that the hoops are correctly positioned, and that the machine is not pulsed at high field while the hoops are hot from a bake-out. Fatigue might be a problem since we have so much periodic stress, but we won't be running at maximum field most of the time, and given our usual usage it will be a couple of years before that sort of problem should show up, if at all. While not a conservative design by the standards of bridge or building construction, we have provided sufficient safety margin for our application.

The detailed design of the inner and outer hoops is shown in figs. 13 and 14, respectively.

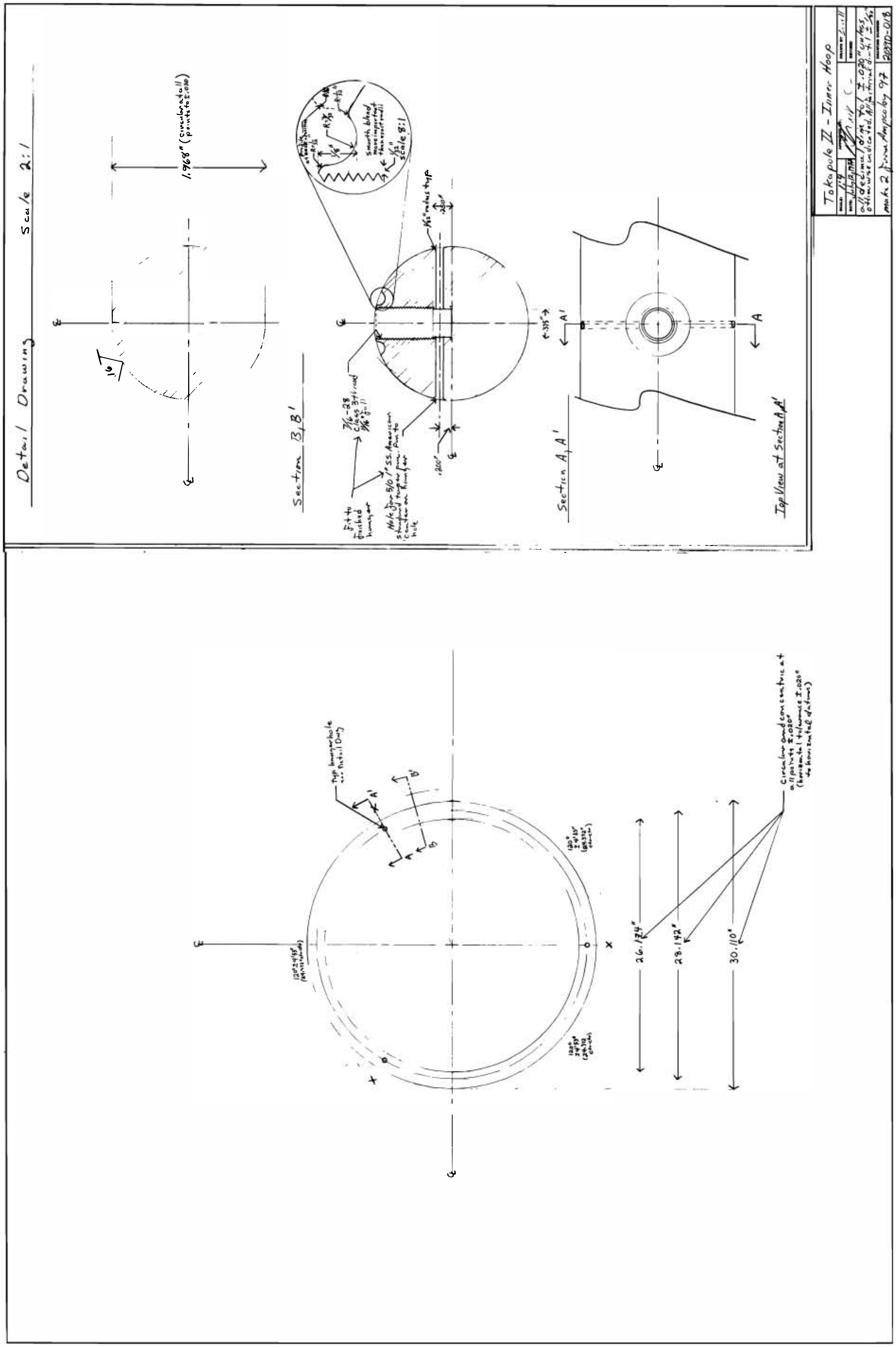
Detail Drawing
Scale 2:1
Section B,B'
Section A,A'
Top View at Section A,A'
Tokapole II - Inner Hoop
26.174"
28.142"
30.110"

Figure 13

VII. TOROIDAL FIELD

Assuming 30 - 240μF 5kV capacitors are used for the poloidal field, we will have 42 such capacitors left to energize the toroidal field. The single turn inductance of the toroidal gap (neglecting the small amount of flux excluded by the hoops) is

$$L = \frac{\mu_o H}{2\pi} \ln \frac{R_2}{R_1} \cong 0.083 \ \mu\text{hy}.$$

The leakage inductance is difficult to estimate, but in Tokapole I with a 48-turn winding and a 4.2 msec half-period with 24 capacitors, the total single turn inductance is about twice the value calculated in the above manner. If we make the pessimistic assumption that Tokapole II will also have a coupling coefficient of 0.5, then the single turn inductance is 0.166 μhy.

The 30° port spacing allows 24 toroidal field windings at equally spaced intervals where the winding crosses the gap at the outer circumference of the lid. An acceptable toroidal field coil would then have an integral multiple of 24 turns. The half-periods obtainable with 42 capacitors for various numbers of turns are given below:

N	T (msec)
24	3.08
48	6.17
72	9.25
96	12.34

The 96-turn case was chosen since it gives a period comparable to that of the poloidal field and since four turns will fit nicely in a square cross section channel. Since it will be easier to wind the coil in two 48 turn segments, we might want the flexibility of operating them either in series (12.34 msec) or in parallel (6.17 msec). The smaller turns ratio might also be desirable if we later wish to enlarge our capacitor banks without lengthening the period.

The largest channels that can conveniently fit between ports will accomodate four wires of ~7/8" diameter with insulation. For reasonable insulation, the largest wire size is AWG 4/0. The wire chosen for the toroidal field winding is fine stranded (2100 strands of #30), copper, NEC type flexarr insulation, rated for 600V and 150° C. with a nominal OD of 0.830". A sample of the wire survived a 1 hour bake in an oven at 260° C. The total required winding length is ∿710 ft., and the dc resistance is 8.7 mΩ for the parallel connection and 34.8 mΩ for the series connection. Using the same formula as for the poloidal field winding,

$$\frac{\Delta U}{U} = \frac{RT}{2N^2L} = \begin{cases} 7.02\% \text{ for } T = 6.17 \text{ msec} \\ 14.04\% \text{ for } T = 12.34 \text{ msec,} \end{cases}$$

where U is the total magnetic energy including leakage.

The transmission line is assumed to consist of a twisted pair of 40' long #4/0 wires and to have a dc resistance of 3.92 mΩ. The energy loss is

$$\frac{\Delta U}{U} = \frac{RT}{2N^2L} = \begin{cases} 3.16\% \text{ for } T = 6.17 \text{ msec} \\ 1.58\% \text{ for } T = 12.34 \text{ msec.} \end{cases}$$

In addition to these losses, there are losses produced by the currents that flow on both the inside and the outside of the vacuum vessel and the currents that flow the short way around each hoop. As in the case of poloidal field losses, these losses can be estimated from

$$\frac{\Delta U}{U} = \frac{FRT}{2L}$$

The currents are assumed to flow over a skin depth which is taken as 1.09 cm. for the 6.17 msec pulse and 1.54 cm. for the 12.34 msec. pulse in 6061 aluminum and 0.8175 cm. for the 6.17 msec. pulse and 1.155 cm. for the 12.34 msec. pulse in Ampcoloy97 copper. F was taken as unity for the inside walls and hoops and for the outside of the inner wall. The resistance (FR) of the outside of the top, bottom, and outer walls was assumed the same as the outside of the inner wall despite the larger area because of the non-uniform current distribution. The results of the calculation are summarized in Table VII. Of the 126 kJ available from the capacitors, about 25 kJ is lost in resistances, about 50 kJ is stored in fields outside the tank, and about 50 kJ is stored as field inside the vacuum vessel.

The magnetic field on axis is given in terms of the field energy inside the toroid (U_o) by

$$B_o = \frac{1}{R_o}\sqrt{\frac{\mu_o U_o}{\pi H \ \ln R_2/R_1}}$$

and is equal to 4.4 kG for 50 kJ of energy stored in the field. To produce this field, 1552 kA-turns are required.

The electrical representation of the toroidal field primary circuit is shown below:

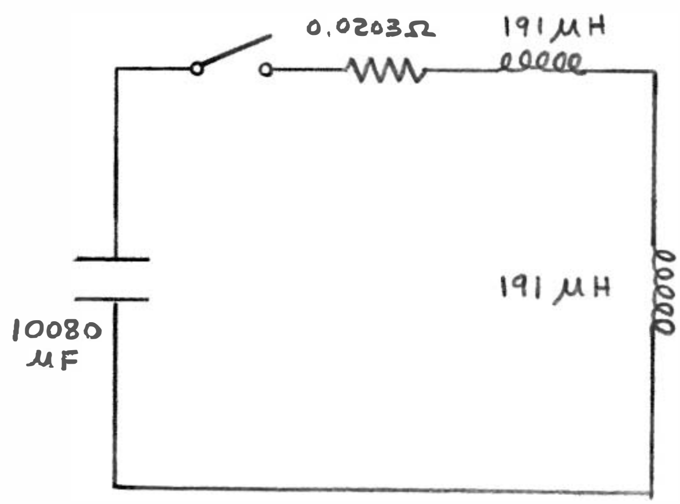

6.17 msec half-period

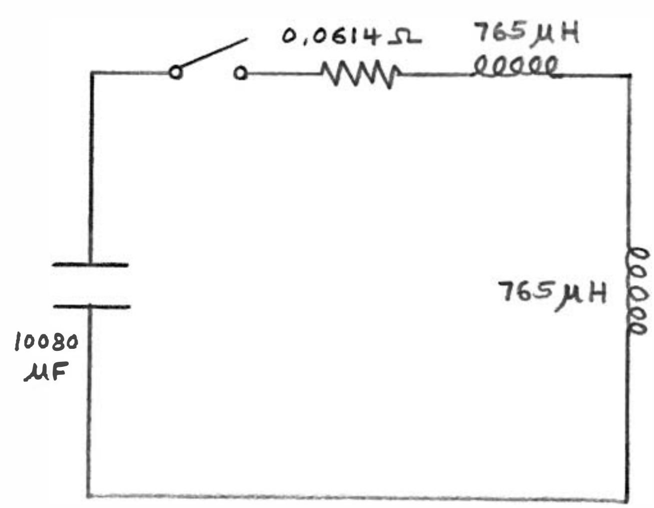

12.34 msec half-period

TABLE VII.

SUMMARY OF TOROIDAL FIELD ENERGY LOSSES

	6.17 msec		12.34 msec	
	$\Delta U/U$ (%)	ΔU (kJ)	$\Delta U/U$ (%)	ΔU (kJ)
transmission line	3.16	3.42	1.58	1.60
primary	7.02	7.60	14.04	14.21
inside inner wall	0.72	0.78	1.03	1.04
inside top wall	0.43	0.47	0.62	0.63
inside bottom wall	0.43	0.47	0.62	0.63
inside outer wall	0.28	0.30	0.40	0.40
outside inner wall	0.81	0.88	1.17	1.18
outside top wall	0.81	0.88	1.17	1.18
outside bottom wall	0.81	0.88	1.17	1.18
outside outer wall	0.81	0.88	1.17	1.18
UI hoop	0.34	0.37	0.48	0.49
LI hoop	0.34	0.37	0.48	0.49
UO hoop	0.19	0.21	0.27	0.27
LO hoop	0.19	0.21	0.27	0.27
total loss	16.34	17.70	24.47	24.77
energy available	116.34	126.00	124.47	126.00
field energy inside	50.00	54.15	50.00	50.61

The L/R time for the two cases is 18.8 and 24.9 msec. A power crowbar would need 656 or 993 volts respectively at peak field to overcome the losses for the two winding configurations. The electrical Q for the two cases is 9.59 and 6.34. The reverse swing of the voltage should leave the capacitors charged to 4.24 kV and 3.90 kV respectively for an initial charge of -5 kV. It might be desirable later to try to recover some of this energy to reduce the charging time.

We will now estimate the force exerted per unit length on each tie-down channel. Each channel is assumed to contain 4-7/8" diameter wires in a square array and the current is assumed to be concentrated at the center of that array. The mutual attraction is ignored, and the repulsion is assumed to be caused by an identical current imaged about a plane one skin depth into the aluminum. The distance between the current and its image is calculated to be 6.625 cm. for the 6.17 msec. pulse and 7.525 cm. for the 12.34 msec. pulse. For 1552 kA in the tank, each channel carries 64,667 amps, and the force/unit length is 76.5 lb/inch for the 6.17 msec pulse and 63.5 lb/inch for the 12.34 msec. pulse. Taking the worst case and extrapolating to an eventual 10 kG on axis, the force is ~200 lbs/inch. Considering rebound, the pulsed force could be as much as 1.7 times higher or ~340 lbs/inch.

In order to calculate the strength of the channels, first the second moment of area I must be determined. By the method of "Marks Standard Handbook for Mechanical Engineers" (7th ed., McGraw-Hill, 1967):

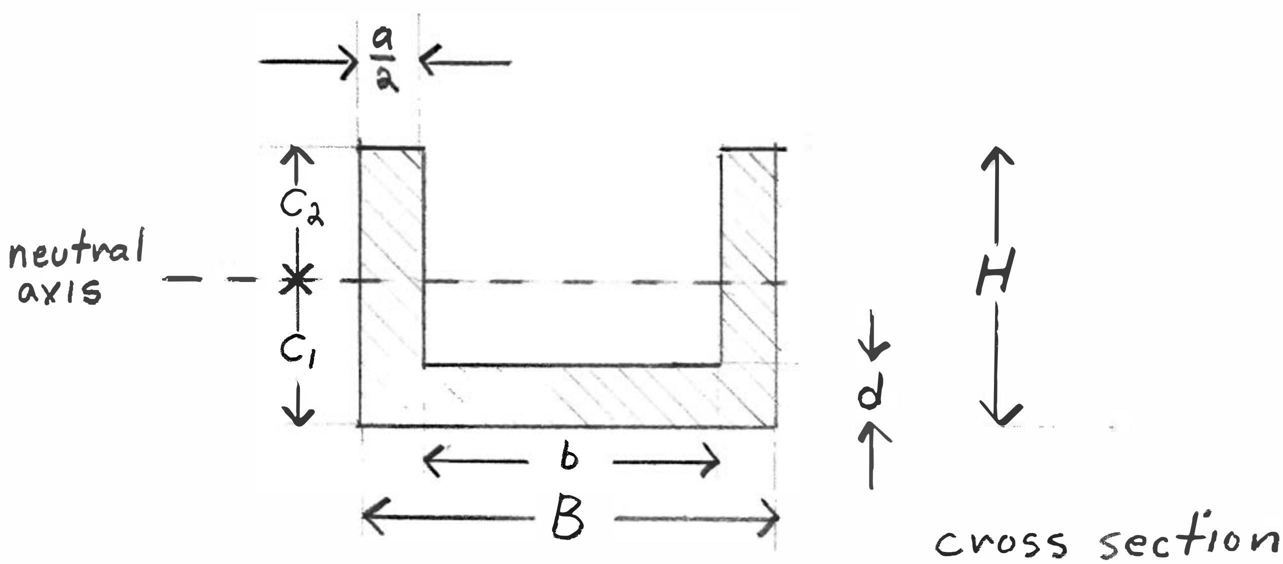

$$I = \frac{Bc_1{}^3 - bh^3 + ac_2{}^3}{3}$$

$$C_1 = \frac{aH^2 + bd^2}{2(ah + bd)}$$

$$C_2 = H - C_1$$

$$h = C_1 - d$$

For a 2 × 1 3/4 × 1/8" channel,

$a = 1/4 \qquad H = 1\ 3/4 \qquad B = 2 \qquad b = 1\ 3/4 \qquad d = 1/8$

$C_1 = 6.04 \times 10^{-1}$

$C_2 = 1.146$

$h = 4.79 \times 10^{-1}$

$I = 2.08 \times 10^{-1}$

$I/C_1 = 3.45 \times 10^{-1}$

Next we apply the beam formula to get the bending moment:

$$M_b = \frac{w\ell^2}{8}$$

w = distributed load (lbs./in.)

ℓ = beam span

$$\frac{M}{\sigma} = \frac{I}{C}$$

σ = stress

$$\therefore \quad \frac{w\ell^2}{8\sigma} = \frac{I}{C} \qquad \ell = \sqrt{\frac{I8\sigma}{cw}}$$

The channel is 6063-T52 aluminum, so σ_{max} = 43,000 psi. If w = 340 lb./in., then ℓ = 18.68". This is the maximum allowable distance between hold down bolts. There is also a shear strain at the held down section. To allow for this and a safety factor, it seems reasonable to legislate a maximum of ∿10" between hold downs.

Some of the ends of the channels will be free (i.e., rather than a beam with two supports, it will be a cantilever). In this case $Mb = \frac{w\ell^2}{2}$, so our previous maximum needs to be divided by 2, giving a maximum exposed length of ∿5".

To estimate the forces on the hold down studs we consider the case of a pair of hold down studs near the end of a channel.

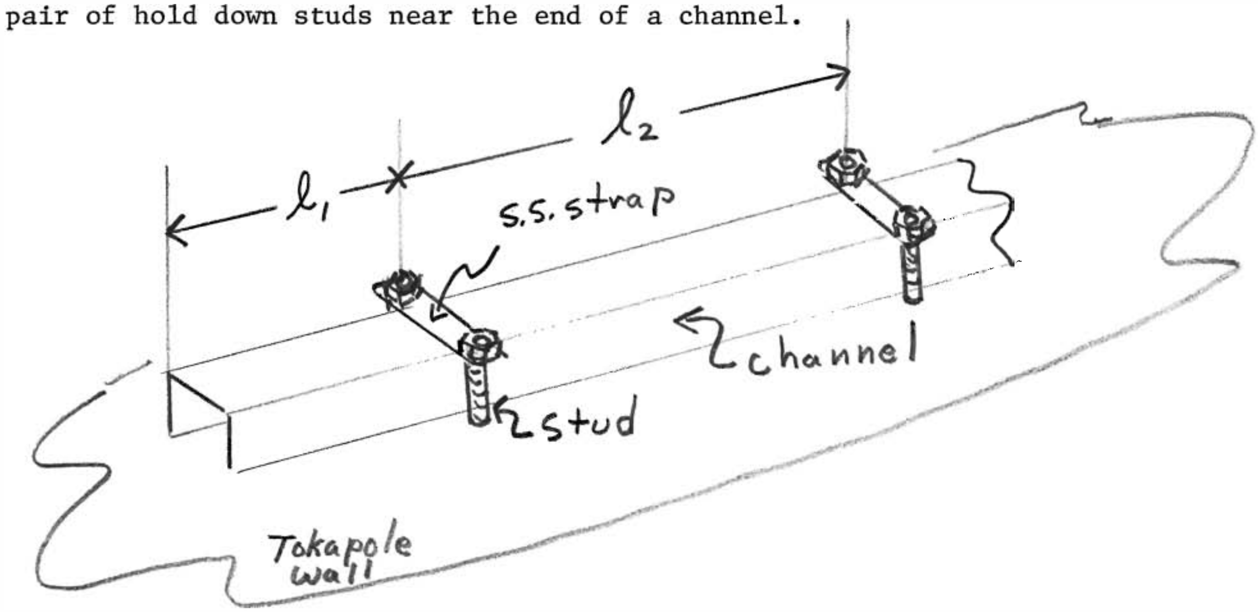

Suppose further that all the spans were maximum (ℓ_1 = 5", ℓ_2 = 10"). Another pair of studs supports half of the load on span ℓ_2, so $W = \frac{w\ell_2}{2} + w\ell_1 = 3{,}400$ lbs. Since there are two bolts, the load per bolt is $\sim$1,700 lbs. If we use 3/8-24 studs they have a tensile area, A_ε, of 0.088 in.^{2}, and so

$$\sigma = \frac{W}{At} = 19{,}320 \text{ psi.}$$

A minimum yield stress for stainless steel is about 30,000 psi, so we have a comfortable safety margin.

By the same method as Section IV, the thread engagement length necessary was found to be 0.600". Holes tapped 3/4" deep ought to have a decent safety margin.

ACKNOWLEDGEMENTS

We are indebted to a large number of people who made helpful suggestions throughout the design of Tokapole II. We profited particularly from discussions with D. W. Kerst, K. R. Symon, S. C. Prager, and R. Vallem. Most of the construction was done at the U.W. Physical Sciences Laboratory under the capable direction of L. C. Thomas and G. Henderson. Graduate students who assisted in the planning and construction include R. Groebner, D. Holly, A. Biddle, B. Lipschultz, D. Witherspoon, T. Osborne, D. Shepard, and M. Sengstacke.